Potential Use of Remote Sensing to Support the Management of Freshwater Fish Habitat in Canada

James V. Marcaccio, Jesse Gardner Costa, and Jonathan D. Midwood

Fisheries and Oceans Canada
Ontario and Prairie Region
Great Lakes Laboratory for Fisheries and Aquatic Sciences
867 Lakeshore Road
Burlington, ON L7S 1A1

2022

Canadian Technical Report of Fisheries and Aquatic Sciences 3424

Fisheries and Oceans Canada | Pêches et Océans Canada

Canada

Canadian Technical Report of Fisheries and Aquatic Sciences

Technical reports contain scientific and technical information that contributes to existing knowledge but which is not normally appropriate for primary literature. Technical reports are directed primarily toward a worldwide audience and have an international distribution. No restriction is placed on subject matter and the series reflects the broad interests and policies of Fisheries and Oceans Canada, namely, fisheries and aquatic sciences.

Technical reports may be cited as full publications. The correct citation appears above the abstract of each report. Each report is abstracted in the data base *Aquatic Sciences and Fisheries Abstracts*.

Technical reports are produced regionally but are numbered nationally. Requests for individual reports will be filled by the issuing establishment listed on the front cover and title page.

Numbers 1-456 in this series were issued as Technical Reports of the Fisheries Research Board of Canada. Numbers 457-714 were issued as Department of the Environment, Fisheries and Marine Service, Research and Development Directorate Technical Reports. Numbers 715-924 were issued as Department of Fisheries and Environment, Fisheries and Marine Service Technical Reports. The current series name was changed with report number 925.

Rapport technique canadien des sciences halieutiques et aquatiques

Les rapports techniques contiennent des renseignements scientifiques et techniques qui constituent une contribution aux connaissances actuelles, mais qui ne sont pas normalement appropriés pour la publication dans un journal scientifique. Les rapports techniques sont destinés essentiellement à un public international et ils sont distribués à cet échelon. II n'y a aucune restriction quant au sujet; de fait, la série reflète la vaste gamme des intérêts et des politiques de Pêches et Océans Canada, c'est-à-dire les sciences halieutiques et aquatiques.

Les rapports techniques peuvent être cités comme des publications à part entière. Le titre exact figure au-dessus du résumé de chaque rapport. Les rapports techniques sont résumés dans la base de données *Résumés des sciences aquatiques et halieutiques.*

Les rapports techniques sont produits à l'échelon régional, mais numérotés à l'échelon national. Les demandes de rapports seront satisfaites par l'établissement auteur dont le nom figure sur la couverture et la page du titre.

Les numéros 1 à 456 de cette série ont été publiés à titre de Rapports techniques de l'Office des recherches sur les pêcheries du Canada. Les numéros 457 à 714 sont parus à titre de Rapports techniques de la Direction générale de la recherche et du développement, Service des pêches et de la mer, ministère de l'Environnement. Les numéros 715 à 924 ont été publiés à titre de Rapports techniques du Service des pêches et de la mer, ministère des Pêches et de l'Environnement. Le nom actuel de la série a été établi lors de la parution du numéro 925.

Canadian Technical Report of
Fisheries and Aquatic Sciences 3424

2022

Potential use of remote sensing to support the management of freshwater fish habitat in Canada

by

James V. Marcaccio, Jesse Gardner Costa, and Jonathan D. Midwood

Fisheries and Oceans Canada
Ontario and Prairie Region
Great Lakes Laboratory for Fisheries and Aquatic Sciences
867 Lakeshore Road
Burlington, ON
L7S 1A1

Cat. No. Fs97-6/3424E-PDF ISBN 978-0-660-37849-7 ISSN 1488-5379

Correct citation for this publication:

Marcaccio, J.V., Gardner Costa J., and Midwood J.D., 2022. Potential use of remote sensing to support the management of freshwater fish habitat in Canada. Can. Tech. Rep. Fish. Aquat. Sci. 3424: ix + 56 p.

TABLE OF CONTENTS

LIST OF TABLES

LIST OF FIGURES

ABSTRACT

Marcaccio, J.V., Gardner Costa J., and Midwood J.D. 2022. Potential use of remote sensing to support the management of freshwater fish habitat in Canada. Can. Tech. Rep. Fish. Aquat. Sci. 3424: ix + 56 p.

Remote sensing (RS) is the study of the Earth's surface through image data captured from a distance using satellite- or airborne-based sensors. These datasets acquire detailed and accurate information over large continuous swaths that can cover a variety of spatial (<0.1 m – 1000 m pixel) and temporal (<1 day to 2 week revisit; historically from ~1950s) resolutions. At its most basic RS can include simple observation of images. Through techniques presented herein, RS can be used to map land cover classes such as vegetation and substrate, track changes in habitat area stream channels, and measure local factors that may influence habitat aquatic connectivity within a watershed, among many other applications. Effective use of RS can reduce the need for in-person site visits and increase the geographic and temporal scale of habitat mapping to support management of freshwater habitat resources. With specific focus on the Fish and Fish Habitat Protection Program of Fisheries and Oceans Canada, this report identifies the types of projects or project end-points that could benefit from RS, discusses considerations related to planning and conceiving a RS project, and outlines a workflow that can help determine if RS would benefit a project and the steps needed for implementation.

RÉSUMÉ

Marcaccio, J.V., Gardner Costa J., and Midwood J.D. 2022. Potential use of remote sensing to support the management of freshwater fish habitat in Canada. Can. Tech. Rep. Fish. Aquat. Sci. 3424: ix + 56 p.

La télédétection est l'étude de la surface de la Terre à partir de données d'images recueillies à distance par des capteurs satellitaires ou aéroportés. Ces ensembles de données permettent la collecte d'informations détaillées et précises sur de grandes étendues continues qui peuvent couvrir une variété de résolutions spatiales (pixels de < 0,1 m à 1 000 m) et temporelles (observation du même point de < 1 jour à 2 semaines; depuis les années cinquante environ). Dans sa forme la plus élémentaire, la télédétection peut consister en une simple observation des images captées. Grâce aux techniques présentées ici, la télédétection peut entre autres être utilisée pour cartographier les classes de la couverture terrestre, comme la végétation et le substrat, pour faire le suivi des changements qui surviennent dans les cours d'eau d'une zone d'habitat, et pour mesurer les facteurs locaux susceptibles d'influencer l'habitat, comme la connectivité aquatique d'un bassin versant. L'utilisation efficace de la télédétection peut réduire la nécessité d'effectuer des visites sur place et augmenter l'échelle géographique et temporelle de la cartographie des habitats pour faciliter la gestion des ressources d'eau douce. Ce rapport, qui met l'accent sur le Programme de protection du poisson et de son habitat de Pêches et Océans Canada, cible les types ou les paramètres de projets susceptibles de tirer avantage de la télédétection, aborde des considérations relatives à la planification et à la conception d'un projet de télédétection, et décrit un flux de travail permettant de déterminer si la télédétection bénéficierait à un projet et quelles seraient les étapes nécessaires à sa mise en œuvre.

LIST OF ABBREVIATIONS

Acronym	Definition
DEM	Digital Elevation Model. A raster dataset that represents the verticality of the earth's surface, and commonly used to describe either a DTM or DSM. There is no consistent definition between DEM, DTM, and DSM, though this is the most common delineation between each and as such these definitions will be used in this document.
DN	Digital Numbers; raw data output from a RS sensor
DSM	Digital Surface Model. A raster dataset representing the verticality of the earth's surface including all objects on it.
DTM	Digital Terrain Model. A raster dataset representing the verticality of the earth's bare ground surface (without objects like plants or buildings).
EM	Electromagnetic, as in spectrum
HH, VV, HV, VH	H = horizontal, V = vertical. Energy polarizations for radar systems. The first letter indicates the plane on which the energy is sent from the system, the second letter indicates the plane on which the energy is received by the system. HH and VV are deemed to be 'like-polarized', while HV and VH are cross-polarized.
LULC	Land-use, Land cover.
NADIR	Direction pointing directly below an observer. Can be mathematically represented as the negative Z-axis from an observer's position.
NDVI	Normalized Difference Vegetation Index, Rouse et al. 1973. Represented by ((NIR - Red)/(NIR + Red)). NDVI shows the photosynthetic capacity of the object, where dense, growing vegetation has a larger response.
NIR	Near-infrared
RGB	Red, green, blue; commonly refers to sensors that span the visible spectrum of energy
RS	Remote Sensing
SAR	Synthetic Aperture Radar
SR	Surface Reflectance; a correction applied to RS data that gives values equivalent to the energy at the surface of the earth (before rebounding off of the surface into the atmosphere)
SWIR	Short-wave infrared
TOA	Top of Atmosphere; a correction applied to RS data that gives values equivalent to the energy transmitted through the earth's atmosphere (after rebounding off of the surface)
UAS	Unmanned autonomous system or unmanned aerial system. All equipment required for operation of a 'drone' (e.g. controller, radio, flight system), including the drone itself.
UAV	Unmanned autonomous vehicle, or unmanned aerial vehicle. Commonly referred to as 'drone'; separate from UAS in that it only refers to the vehicle itself.

INTRODUCTION

Remote sensing (RS) can be broadly defined as a method to obtain information without direct access to it, such as the human senses of sight, smell, and hearing. In a modern context, RS refers to utilizing airborne or space-borne sensors that capture information on a planet, most commonly Earth. These systems allow researchers to capture targeted and accurate data of Earth's atmosphere and surface properties with collected data covering a wide electromagnetic spectrum.

Remote sensing data are continuous across the area they cover and are composed of multiple 'bands' of data corresponding to the wavelength of energy they analyze (e.g., visible red, ultraviolet). These data are captured by image sensors that can be mounted on a variety of platforms. The data produced via each method are largely the same (i.e., pixel-based data 'sheets') and the platform to be used is based on project requirements and objectives. Once data are collected, they must be processed in software capable of handling RS data and analyses. While many GIS software have this capability (e.g., ArcGIS, QGIS), dedicated RS software often have more tools and streamlined analyses specifically tailored for RS data. With increased computer processing power and cloud-based software, new RS techniques are constantly being developed and tested at larger scales. It is important to note that while these components are reviewed in this document individually, most RS projects will utilize many techniques in tandem to obtain the desired outputs.

There are myriad applications of RS including ecological uses (Pettorelli et al. 2016) and those related to measuring and monitoring fish habitat (Dauwalter et al. 2017). RS can complement or enhance established fish habitat science and monitoring but also has several advantages unique to its field. RS can be used for large-scale and/or long-term monitoring of fish habitat and the surrounding landscape without the need for time-specific field work. Users can acquire date-specific image data for monitoring changes in fish habitat and perform RS analyses to measure changes in physical habitat features such as vegetation and substrate cover or composition, changes in habitat area or stream channels, and changes in local factors that may influence habitat such as soil moisture (represents drainage) or land cover within a watershed. RS provides a reproducible approach to analyze fish habitat at local, regional, or even national scales without incurring significantly more processing time. The objective of this report is to review available RS platforms and their associated features, the types of RS data, commonly used software packages for working with and analyzing RS data, and the types of analysis that can be done with collected RS information. The report begins with recommendations on how RS sensors, techniques, and derived products can be applied to support the management of freshwater fish habitat with specific focus on the Fish and

Fish Habitat Protection Program at Fisheries and Oceans Canada. RS has many common terms and acronyms that may be confusing and unfamiliar to those that do not have experience in the topic; a list of these can be found on page ix.

CONSIDERATIONS FOR FFHPP TO EMPLOY REMOTE SENSING (RS)

The Fish and Fish Habitat Protection Program (FFHPP) at Fisheries and Oceans Canada is responsible for administration of the Fisheries Protection Provisions in the *Fisheries Act* and the *Species at Risk Act* for aquatic species. As such, the Program is responsible for assessing impacts from development on fish and fish habitat and protecting fish and fish habitat throughout Canada. Given the scale of this requirement, RS-related techniques and derived products would benefit this Program since RS provides a reproducible approach to map fish habitat at local, regional, or even national scales. With RS, users can acquire date-specific image data for monitoring changes in fish habitat and perform RS-specific analyses to measure changes in physical habitat features within a watershed. FFHPP can leverage these techniques to enforce their mandate under the *Fisheries Act*, specifically subsections 34.1 (1)(d), *"the cumulative effects of the carrying on of ... works, undertakings or activities that have been or are being carried out on, on fish and fish habitat"*, and (f), *"whether any measures and standards to offset the harmful alteration, disruption or destruction of fish habitat give priority to the restoration of degraded fish habitat"* (Minister of Justice 2020). If the goals and objectives for a RS-project are defined, DFO science and spatial data management groups can help develop RS workflows that can be applied across a range of projects and can help create tools to inform regulators reviewing in-water projects. The RS-related subsections outlined in this report describe in detail the types of imagery that can be acquired, the techniques that can be applied to this imagery, and the software platforms that are best suited to apply these techniques. In this section, we summarize some key messages from the overall document, identify the types of projects or project end-points that could benefit from RS, outline a workflow that can help FFHPP determine if RS would benefit their project, discuss considerations related to planning and conceiving of a RS project and the steps needed for implementation, and conclude with an overview of specific elements contained within this document that may be of interest to FFHPP.

KEY MESSAGES

Overall

- Remote sensing can be used to acquire detailed and accurate information over large continuous swaths of the Earth's surface.
- Effective use of remote sensing can reduce the need for in-person site visits and increase the geographic and temporal scale of habitat mapping and protection.

- More complex uses of remote sensing are likely appropriate for large-scale projects or for internal documentation that requires coverage of a large spatial area (e.g., State of Habitat reporting, program review, assessment of cumulative changes in an area).
- Large spatial coverage supports mapping and evaluation of watershed-scale changes, which can help develop our understanding of the cumulative effects of development activities on fish and fish habitat.

Remote sensing software

- Remote sensing makes use of software that is often bundled in existing Geographic Information Systems but more specialized software, which can streamline analyses or conduct more advanced analyses where available (see "Remote Sensing Software" section).
- Remote sensing makes use of software that is often open source and reproducible, so the methods and workflow applied in one project can be applied to others at local, regional, or even national scales without incurring significant development time resulting in faster processing.

Remote sensing data

- Many remote sensing platforms exist (satellites, plane-based photography, unmanned aerial vehicles) that offer differing spatial (<0.1 m – 1000 m pixel) and temporal (<1 day revisit – 2-week revisit; historically from ~1950s) resolution with unique data captured (e.g., only visible spectrum light, infrared, microwave; see "Remote Sensing Sensors and Platforms" section).
- Fisheries and Oceans Canada can leverage existing freely available data that routinely cover the Earth's surface (e.g., Landsat and Sentinel satellites - recapture imagery every ~2 weeks; the RADARSAT program is owned by the Government of Canada).

Remote sensing techniques

- Object-oriented image clustering or classification, wherein computer software merges pixels with similar properties into an object (see "Remote Sensing Techniques: Image Classification: Object Oriented" section), is a useful technique for FFHPP. This technique substantially reduces the burden of processing and identification on the user since there are fewer objects that require classification and boundaries between features tend to be well defined. This technique is especially critical for the new wave of high-resolution remote sensing data where pixels <1 m in size can lead to files that are millions of pixels and form multi-gigabyte files. This technique has been used to map fish habitat features including vegetation (Midwood and Chow-Fraser 2010), wetland

inundation dynamics (Wu et al. 2019), and riverine habitat depth and substrate type (Hugue et al. 2016).

- Change detection, which can be accomplished a variety of ways (see “Remote Sensing Techniques: Change Detection” section), is a useful technique for FFHPP since it can contrast the location and coverage of features of interest between two time periods. This can help determine whether offsetting projects have been successful (e.g., riparian planting survival, created open water habitat meets area targets, desired changes to a system are maintained throughout monitoring timeline, or physical habitat has not shifted due to wind/wave action).

MEASURABLE END-POINTS OR PROJECTS THAT CAN BENEFIT FROM RS

Pathways of effects (PoE) is a decision-support tool used by management sectors of Fisheries and Oceans Canada to support Ecosystem-Based Management (Government of Canada 2012). It can be used to determine how anthropogenic activities in or near water may affect an ecological or biological endpoint related to fish and fish habitat. An essential element of a PoE is the selection of measurable endpoints, which are indicators that are used to measure or track changes through time. These endpoints need to be well-defined, meaningful, practical, and easily understood and can generally be broken down into two components: an ecological entity (i.e., what in the environment is changing) and a measurable attribute of that entity (i.e., what about the entity is changing; Government of Canada 2012). Given their utility to the management sectors within Fisheries and Oceans Canada and the quantitative nature of their requirements (which links well with RS techniques), here we identify fish habitat-related ecological entities that can be mapped using RS and their associated measurable attributes. When combined, these can provide a measurable endpoint that can be useful within the PoE framework as well as for works focused on assessing the extent and condition of fish habitat. For example, ecological entities and measurable attributes are conceptually similar to indicators and metrics as defined by the State of Fish and Fish Habitat in Canada reporting initiative that is underway at the time of writing.

To inform selection of the ecological entities that are listed in Table 1, we drew on the different components of fish-habitat paradigms outlined in Minns and Wicheret (2005). In that work they discuss an “older” paradigm focused on depth, cover, and substrate as measures that relate to fish density or biomass, and a “newer” paradigm formed around thermal, motion (i.e., hydrodynamics), and optical regimes that links to growth, survival, movement, and egg deposition (among other life history components). Additional ecological entities were added based on other biological, physical, or limnological features that may influence fish and fish habitat and have been demonstrated as map-able entities in previous works. Dauwalter et al. (2017) provide an overview of studies that have applied RS technology to map many of these features and here we provide a similar summary in Table 1 with a focus on measurable attributes for fish habitat.

Table 1: *List of ecological entities related to fish habitat and their associated measurable attributes that can be mapped or tracked using remote sensing approaches. For anything that is mapped, distribution (where it is situated spatially), area (surface area), and heterogeneity (variety of classes within a defined area) are measurable attributes for all ecological entities and are therefore not listed. Further, while this table shows the range of attributes that can be mapped, it is by no means exhaustive.*

Ecological entity	Measurable attribute
Vegetation	Species; Cover; Height
Woody Debris/Structure	Cover; Height
Substrate	Composition
Topography	Depth; Elevation; Slope
Temperature	Surface Water; Land; Temperature Variability; Growing Degree Days
Light	Turbidity; Water Clarity
Motion (hydrodynamics)	Fetch; Flooding; Stream Alterations
Connectivity	Distance to Proximate Habitats; Number of Connections
Primary Production	Net Primary Productivity; Chlorophyll-
Watershed Condition	Land Cover Type; Changes in Land Cover
Ice	Cover; Type; Thickness
Geomorphology	Connectivity; Channel Morphology

With these ecological entities and measurable attributes in mind, what follows is a list of examples of projects that can combine measurable attributes with remote sensing techniques (presented in detail in the “Remote Sensing Techniques” section) to support management of freshwater fish habitat.

- Mapping habitat features of interest (e.g., vegetation, substrate) and calculating their area of coverage
- Compiling information on habitat conditions (e.g., stream length or width, connectivity of aquatic habitat, shoreline complexity of lakes)
- Measuring changes in habitat area of cover, condition, or type through time
- Developing digital elevation models on land (to support evaluation of changes in overland flow or connectivity caused by a project) and in water (bathymetry)
- Measuring cumulative changes in an area of interest (e.g., where multiple separate projects may be proposed or underway)
- Evaluating the un-intended consequences of a project (e.g., channelizing a stream may change wetted areas within the watershed away from project area)
- Complement regular monitoring and reporting for large-scale projects
- Supporting documentation of reported occurrences (e.g., can collect pre/post imagery at the site of an occurrence)
- Mapping extent and spread of aquatic invasive plants
- Historic landscape-level analyses where continuous field data do not exist

- Expanding local- and regional-scale data to larger spatial scales (e.g., use field data from a portion of a lake shoreline to map across the entire lake)
- Using the above techniques, detect areas and habitats that would benefit from habitat remediation

RS WORKFLOW AND EXAMPLE

Broadly, the workflow related to using RS products can be split into two phases, project conception and implementation (Figure 1). There are four considerations for the project conception phase that should be reviewed (below) to determine the most appropriate course of action. The implementation phase follows two tracks (Figures 1, 2, 3) where Track 1, *Deriving New Products*, requires more effort and likely the involvement of individuals with RS expertise while Track 2, *Existing Products*, simply involves acquiring existing mapping products. There are advantages and limitations to each track (outlined below) and project objectives as well as availability of the necessary products will dictate the most appropriate path.

Track 1

Project conception phase (Figure 1) – The project team needs to outline specific objectives that they hope to achieve and then determine whether RS is the right approach to meet these objectives; there are four main considerations that will help to guide the project conception workflow:

Timeline when information is required – If the project has a longer timeline (e.g., large-scale, multi-year project) there is potential for the compilation and classification of historic and newly acquired imagery (Implementation Track 1); if urgent, user needs to rely on existing RS-derived products (Implementation Track 2).

Spatial scale – Size of an area of interest will dictate how many images are required, the type of imagery that is available to meet the coverage needed, whether existing imagery is available to meet the required coverage, and the time it will take to process/classify images of interest. Larger areas may not have complete coverage for all platforms (e.g., Landsat 8 has a scene size of approximately 180 km x 185 km, whereas WorldView-3 has a scene size of 66.5 km x 121 km) and will take longer to process/classify.

Temporal scale – Determining the optimal time of year (season) for image collection is linked to the features of interest (e.g., mapping aquatic vegetation should be done in the summer while developing digital elevation models may be best done in winter when vegetation does not obstruct the ground). It should be determined whether a single time period will be sufficient or whether changes through time are of interest (requires multi-year/season imagery).

Features to be mapped – Dictates the type of spectral bands required (e.g., vegetation is distinguishable by absorption of energy in the red band and reflection of energy in the near-infrared band) and the resolution of the imagery (smaller features require higher resolution imagery to accurately map). The types of features to be mapped will also inform the type of analysis that should be completed. For example, in deep waters (>10m) longer wavelengths of light like red and near infrared do not transmit and would not greatly enhance substrate mapping. Conversely, the proportional change in red to near-infrared wavelengths is a strong indicator of plant health and chlorophyll production.

Project implementation phase (Figure 2) – The appropriate imagery needs to be acquired (see "Remote Sensing Sensors and Platforms" section for information on the range of available imagery) and brought into an appropriate software package (see "Remote Sensing Software" section for a review of available packages). The next step is to convert the images created by sensors into distinct land cover classes of interest based on their spectral response; this is generally referred to as *classification* and can be done automatically or with input from the user (see "Remote Sensing Techniques" section for a review of image classification techniques). Some level of validation of the classification is highly recommended and this is typically completed with the aid of reference data that have either been collected in the field or derived from existing mapping products.

Track 2

This track involves the selection of existing data products that may be as simple as reviewing available imagery on Google Earth or downloading products developed and maintained by the Canadian Space Agency, NRCAN, NOAA, or NASA (among many data producers, see Table A1 for potential data sources). Once the correct image is identified, the user can extract the information they need to meet their project objective.

EXAMPLE WORKFLOW

Figure 1 provides an example of a RS project workflow with an objective to measure changes in aquatic vegetation areal cover following the completion of a project that has been authorized by FFHPP (restoration of a small wetland, <10 ha). These authorized works involved the revegetation of a wetland with native vegetation, with actions such as planting of cattails (*Typha* sp.). Conceptualizing the project, we have considered timelines (need the data within several months), spatial scale (<10 ha area), temporal scale (requires multi-year imagery to detect changes in habitat i.e., images from both before and after the project was completed), and the features to be mapped [aquatic vegetation including cattails, common reed, floating vegetation (e.g., white water lilies - *Nymphaea odorata*), and submerged aquatic vegetation (e.g., pondweed - *Potamogeton* spp.)]. For this example, existing mapping products are available;

however, they are of lower resolution (we would prefer <10 m resolution) than we desire for this small area. As such, we need to purchase existing higher resolution imagery and classify the features of interest. Given that we have several weeks to create an RS product, and need to acquire and classify imagery, we will use Implementation Track 1 (Deriving New Products).

Since the focus is on mapping wetland vegetation, images collected during the summer over multiple years with moderate resolution (<10 m) and multi-spectral bands (e.g., red, green, blue, and near-infrared) are required. The object-based classification technique was selected to help combine pixels that contain similar aquatic vegetation classes; these objects can be more accurately mapped since they have defined boundaries and share similar spectral properties (see “Remote Sensing Techniques: Image Classification: Object Oriented” section). Object-based classification requires input and support from a RS specialist, but it has been used extensively in the literature so it can likely be implemented in a matter of weeks. Using semi-automated image classification, the analyst can create a repeatable workflow that will simplify and accelerate the image classification process for the next image. Following this workflow, we have a product made in a few weeks using established techniques that maps the cover of aquatic vegetation that was present in the wetland before and after the authorized works. From these maps, changes in the areal coverage of the aquatic vegetation classes outlined above as well as changes in their distribution within the wetland can be measured and this output can be compared to the original changes proposed in the authorization to ensure targets are being met.

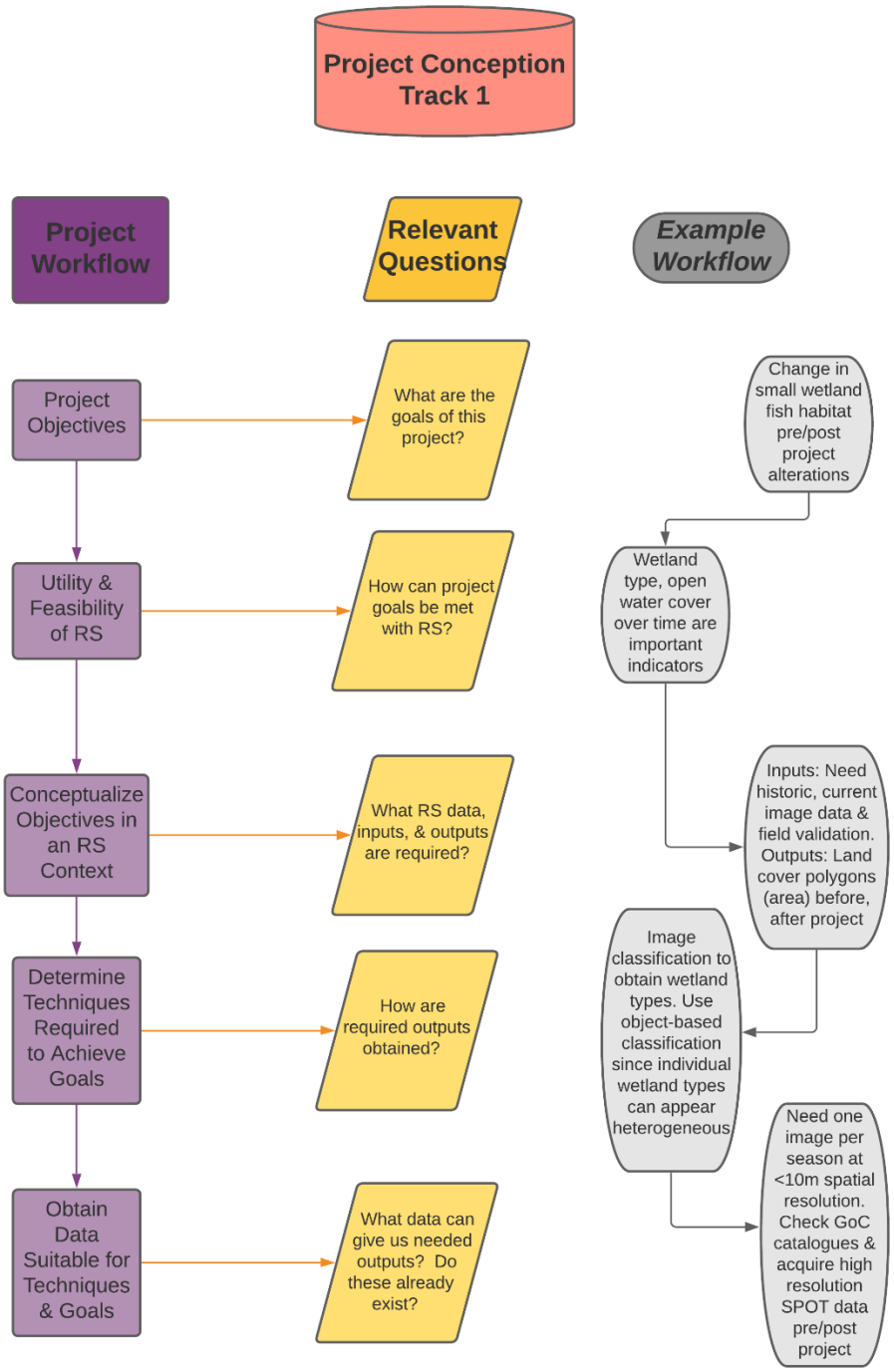

Figure 1. *Project Conception Workflow (Track 1) for use of remote sensing. A theoretical example is on the right (gray boxes).*

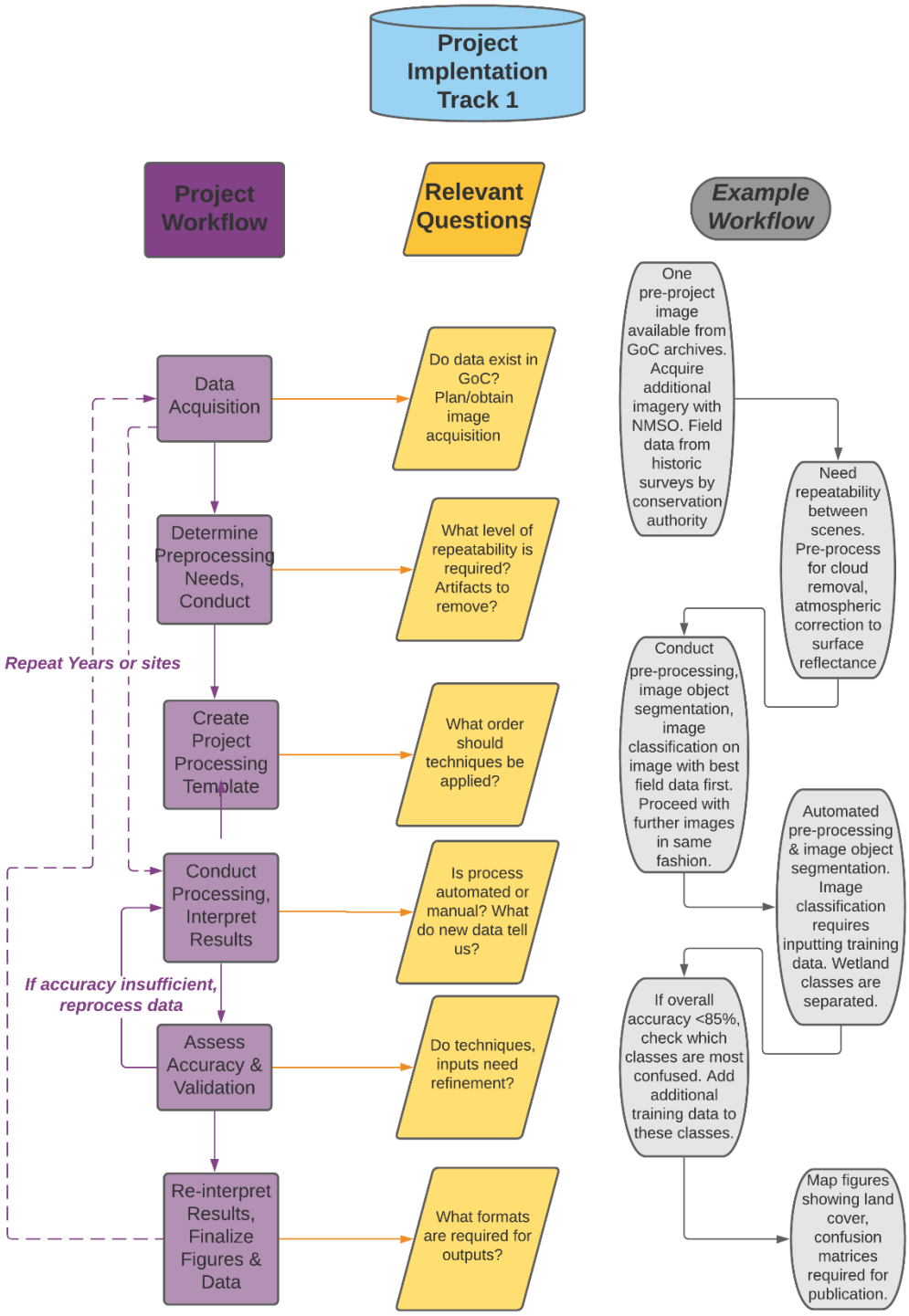

Figure 2. *Project Implementation Workflow (Track 1) for use of remote sensing. A theoretical example is on the right (gray boxes).*

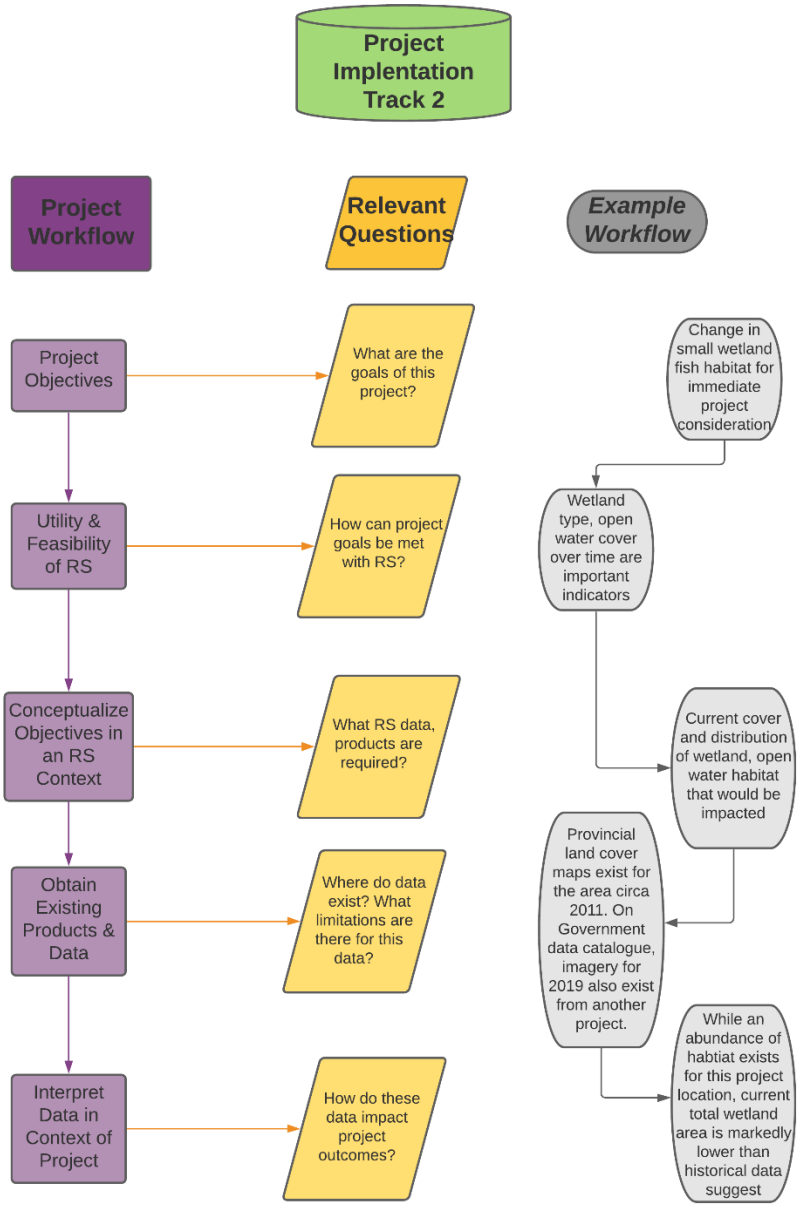

Figure 3. *Project Implementation Workflow (Track 2) for use of remote sensing. A theoretical example is on the right (gray boxes). Note that since this track uses derived remote sensing products, less onus is placed on the user to conduct processing workflows.*

REMOTE SENSING SENSORS AND PLATFORMS

Image sensors are the heart of RS and are what translate light/energy into data that can be analyzed. RS platforms are systems on which these sensors are mounted and can be broadly grouped into three major categories: satellite (space-based), orthophotography (from planes), and unmanned vehicle systems (UVS; also defined as

unmanned aerial vehicles or systems, unmanned autonomous vehicles or systems, or drones). Since the launch of the Landsat series satellites in1972, space-based RS has been the primary data source in the field. These offer near-global coverage and consistent collection of imagery both temporally and spatially. Images acquired within our atmosphere (i.e., from orthophotography and UVS) have much higher resolution than satellite-based products and do not have problems inherent with imaging through the earth's atmosphere (see Active Remote Sensing Platforms section). While there are historic orthophotography datasets available that go back further than satellite-based data, these were not often acquired in a form suitable for more detailed analyses [e.g., not at nadir (point directly below observer), not sufficiently overlapped, and not properly defined geographically]. Orthophotography is limited in geographic scale and significant funds must be allocated when area increases [e.g. the southwestern Ontario Orthophotography project, covering 205,000 km^2, cost over $5,000,000 per acquisition (A. Hogg, Ontario Ministry of Natural Resources and Forestry, personal communication, 2017)]. For UVS, the restrictions and cost of scale are even greater (Marcaccio et al. 2015). For orthophotography and UVS, there are a host of unique sensor and craft combinations that can be employed since the same sensor mounted to different aircraft can change the effective accuracy or spatial resolution of the images collected. This flexibility allows for image acquisition across a broad range of field conditions and project objectives; however, it can also present a challenge since inconsistent image collection parameters can impede both temporal and spatial comparisons. Since orthophotography and UVS datasets are specific to time and place, this report will not go into those platforms in detail. The RS software and techniques described within this document are equally applicable to images from within the atmosphere as well as those outside of it.

There are many historic, current, and future satellite platforms in orbit around Earth. Table A2 lists commonly used platforms and includes the type of data captured as well as launch and decommission date, which define the time period when data from the platform are available. Good historic coverage can be found in the Landsat series platforms (available in true colour + near infrared since 1982), but more recent sensors offer increased temporal resolution (e.g., 1 – 2 day with RapidEye) or spatial resolution (e.g., 30 cm with WorldView-3). A similar table was not generated for orthophotography and UVS since images collected via these platforms are typically project specific with inconsistent spatial and temporal acquisition. For federal government users, the Earth Observation Data Management System (EODMS) contains data from the National Air Photo Library (orthophotography) and other RS data purchased by the Government of Canada. Individual provinces and cities may have their own RS databases such as Land Information Ontario (LIO) and the City of Hamilton GIS database. The platform that is chosen will depend on the parameters required for the project and available budget, with additional spectral bands and higher resolution costing significantly more.

Regardless of platform, imaging sensors can be broken down into passive or active sensors. Passive sensors function much like the human eye or a traditional camera by capturing electromagnetic (EM) radiation reflected off a surface. The source of energy is external to the platform, in most cases the Sun, and the sensor interprets the reflected energy within a defined spectrum. Passive sensors typically include three 'visible' bands that fall somewhere within the red, green, and blue EM spectra (600 – 750 nm, 500 – 560 nm, and 450 – 500 nm range, respectively); when combined these produce an image similar to what we see with our eye. Other wavelengths can be captured with passive sensors, most commonly near infrared (NIR; ~750 – 1000 nm) and short-wave infrared (SWIR; 1000 – 2500 nm) and when combined with the visible spectrum these sensors are typically referred to as multi-spectral. For a list of common RS spectra, see Table A3. Some sensors can be hyper-spectral or ultra-spectral; these have many (often >10) bands that individually cover narrow EM spectra (often ~10 nm). Hyperspectral imaging (HSI) is relatively new in the field of RS and thus few products exist (see Table A2). Many platforms also have a separate panchromatic sensor that acts like black and white film: it accepts a large spectrum of EM in one band, typically across most of the visible spectrum. While panchromatic sensors have coarser spectral resolution, they typically have higher spatial resolution (often ½ or ¼ of the multispectral sensor). The inclusion of this panchromatic sensor can allow post-processing of the coarser multispectral sensors in support of better objective identification (as discussed in the preprocessing section). Passive sensors have been in use for a long time, starting with balloon and aerial film photography. These older datasets may not have well defined metadata or high accuracy but can be important as historic data points. The first satellite based passive sensors for non-military use were launched in the 1970s, providing a rich and continuous dataset. Most recently, technological advances have led to unmanned aerial systems (UAS) being a viable source of high-quality RS data.

While passive sensors measure multiple wavelengths, active systems use a single specific wavelength of energy to record the return or bounce-back of this energy. Since they emit their own energy, these platforms can image during day or night and receive the same data. Active sensors operate at long enough wavelengths (metres to millimetres) that rain, cloud, and other atmospheric properties do not obstruct their imaging. With one single wavelength a system can emit energy that is vertically (V) or horizontally (H) polarized, travelling along an x- or y- axis. The system can then monitor the return of this energy in a like-polarized [e.g., VV (vertical send-vertical receive) or HH (horizontal send-horizontal receive)] or cross polarized (e.g., HV) way, giving three unique configurations [cross polarization returns (HV and VH) are the same regardless of order]. Surface features will give unique responses with different configurations; for example, Bourgeau-Chavez et al. (2015) showed that HV polarized L-band radar is well suited for differentiating emergent wetland vegetation species while the HH derived data are better for open water delineation. When multiple different features are to be mapped, it is therefore preferable to obtain dual polarized imagery (i.e., HH and HV or

VV and VH) when possible, though older systems (such as Radarsat-1) can only operate in single polarization mode. Most active radar platforms do not image at nadir and instead image at an angle, which increases the potential spatial coverage but can cause terrain shadowing and other effects. Relative to passive sensor platforms, there are fewer active sensor platforms in orbit, but Sentinel-1 is publicly available and has been collecting imagery since 2014. The Canadian Space Agency maintains the RADARSAT series satellites (two single satellite missions plus the three satellite RCM) and the data collected by these satellites are available to Government of Canada employees. Radarsat-1 data are also available to the general public. In addition, Government of Canada employees can task the Radarsat satellites (currently restricted to Radarsat-2) in order to obtain optimum imagery over their defined region of interest. This tasking must be coordinated with the Canadian Space Agency through the Government Radarsat Data Services and the Enhanced Management of Orders and Conflicts (EMOC) form.

Most common sensors use RADAR (Radio Detection And Ranging) technology in the microwave spectrum. Multiple sensors within a range of microwave spectra are given the same code (e.g., C-band: 2.75 cm – 7.5 cm). Different microwave spectra generate unique signals from similar land cover, just as visible spectrum passive sensors show different colours for unique land cover. Since active sensors generate their own energy source they can specify the polarization of that energy. Active sensors also include non-imaging devices which include altimeters, scatterometers, and LiDAR (Light Detection And Ranging) products. These are unique in that they generate one-dimensional points of data which can later be interpolated into two- or three-dimensional surfaces. Common uses of these sensors include range detection, elevation determination, and surface properties of materials.

Many sensors exist across a variety of satellite platforms that offer different spatial, temporal, and spectral resolution. Which products to use is dependent on the questions the researcher intends to answer or the outputs an analyst must provide. From a spatial resolution perspective, satellites can be broadly classified as coarse/low resolution (>100 m pixels, like MODIS), medium resolution (10 – 100 m resolution, like Landsat and Sentinel-2) or high resolution (<10 m, such as SPOT). With new advancements in sensor technology and relaxing of satellite regulations, which formerly limited commercial satellite outputs to >30 cm resolution, very high-resolution satellites are coming forward that offer sub-metre spatial resolution. Not all these satellites have fast repeat times, with coverage coming in approximately bi-weekly (Landsat: 10 days), sub-weekly (RADARSAT Constellation: 3 days) and daily (MODIS) intervals. Both temporal and spatial resolution depend on the orbit path and velocity of the satellite which can lead to differing revisit times and spatial resolution dependent on latitude. This is especially true for sensors that image off-nadir as the ‘stretch’ of pixels becomes greater at increasing view angles. Finally, spectral resolution is an area of rapid development; most historic platforms have focused on single wavelengths, three in the visible

spectrum (red, green, and blue), and/or one in the near-infrared region. Recent and future sensors have expanded these limited bands to offer 10 or more wavelengths of observation, commonly called hyperspectral imaging (see 'CHIME'). Increases in resolution of any type come at increased financial cost and maximizing all three can be extremely costly. For each project, the RS analyst should know what spatial, temporal, and spectral resolution is necessary to address their needs a priori to not incur avoidable financial costs.

The field of RS is evolving with rapid advancements in technology and computer processing. There are significant yearly upgrades in satellites, imaging technologies, and software that are allowing innovative and more complex RS projects to proceed. While this list is not exhaustive it does showcase a selection of new and upcoming RS technology that can benefit fisheries research.

RADARSAT CONSTELLATION MISSION (RCM)

As part of Canada's mission to map the Arctic and its ice channels, the Canadian Space Agency (CSA) operates RADARSAT satellites in cooperation with MDA Coroporation (owners of RADARSAT 2). The RADARSAT Constellation Mission (RCM) utilizes three satellites that are smaller than RADARSAT-2, which combined provide a faster repeat cycle (~1 day) than previous missions. The RCM also utilizes circular polarization which can produce and receive any angle of polarization (not just horizontal and vertical); this opens many more opportunities for detailed polarimetric analyses and mathematical manipulations of the data. The RCM was launched in 2019 and became operational later that year. Government employees can task RADARSAT-2 and the RCM to obtain C-band imagery over their area of interest free of charge. Further information and updates can be found at: https://www.asc-csa.gc.ca/eng/satellites/radarsat/default.asp

LANDSAT 9

While the launch date has been pushed back from 2020 to March 2021, Landsat 9 will continue the historical imaging platform of the US Government and continue to offer multi-spectral, medium resolution data on a continuous basis. Landsat 9 has an imaging array similar to Landsat 8 and will be placed in the same orbit as its predecessor. This will decrease the image cycle (~8 days) for global mapping. Landsat 8 should remain operational until 2025 with Landsat 9 providing imaging for an additional 5 – 10 years, though most platforms have far exceeded their operational life expectancy. By the end-of-life of Landsat 8 and 9, the Landsat missions will have provided over 50 years of continuous multispectral imaging. Further information and updates can be found at: https://landsat.gsfc.nasa.gov/landsat-9/

COPERNICUS HYPERSPECTRAL IMAGING FOR THE ENVIRONMENT (CHIME)

Hyperspectral data are incredibly useful tools with very high spectral resolution, but they often cannot achieve high spatial or temporal resolution due to computational costs. These data are also expensive to acquire. The European Space Agency's Copernicus program is planning the launch of the Copernicus Hyperspectral Imaging for the Environment (CHIME) satellite that will supply 20 – 30 m resolution on a 10 – 15 day repeat cycle. CHIME will operate seamlessly between 400 nm (ultra-blue) to 2500 nm (SWIR) in 10 nm increments. If these data are offered as free products (like other Copernicus satellites, e.g. Sentinel-series) this would represent a marked increase in data quality that would be easily accessible for RS. The satellite is planned for launch in the mid-2020s. Further information and updates for CHIME and ROSE-L (below) can be found at:
https://www.esa.int/Applications/Observing_the_Earth/Copernicus/Copernicus_High_Priority_Candidates

RADAR OBSERVING SYSTEM FOR EUROPE L-BAND SAR (ROSE-L)

An additional Copernicus satellite launch is planned for launch in the mid-2020s using L-band SAR. Currently, freely available SAR is only C-band, with the CSA offering historic data from RADARSAT-1 and Copernicus offering Sentinel-1 that is still ongoing. L-band SAR uses a longer wavelength that is more sensitive to wet soil and vegetated areas and can provide better contrast for sea ice determination. The Radar Observing System for Europe (ROSE-L) will use the same orbit as Sentinel-1 and will provide a near-daily repeat cycle in the Arctic and somewhat longer for northern Canada. These data are planned to be of higher resolution than Sentinel-1 (20 m) and should provide a great new dataset to use in Northern regions.

REMOTE SENSING DATA

The primary advantages of RS data are that they cover large geographic ranges and are not discrete across their coverage. In a Geographic Information System (GIS) almost all RS data are 'raster' type data, which are continuous data 'sheets' (in contrast, 'vector' data are discrete). These sheets have pixels (like cells) that are arranged along rows and columns, with the size of the pixel determined by the product used (a function of the sensor's inherent resolution and the distance from sensor to viewing object, usually expressed in metres per pixel). The data value stored in each pixel represents the total reflectance of an object captured by the sensor; more reflectance results in a higher value. Many RS products have multiple 'bands' of data that capture reflectance with a specific energy, which is equivalent to multiple data 'sheets' overlapping each other. The results are concurrent data from multiple bands or wavelengths for a single pixel. How these sensors obtain data is broadly separated into passive and active

sensors, which rely on either an external source of energy (i.e., the sun) or emit their own specific energy, respectively. Raster data will contain more information per unit area than vector data, but this comes with increased processing requirements. Being discrete, vector data does not have to confine itself to a set resolution or grid and can more precisely define boundaries and locations compared to raster data. Some techniques are only available to one data type or the other so even in RS projects it is often necessary to switch between these in order to appropriately address the research question or goal.

RS data are often square (with equal length and width of cells) but can be transformed to other shapes depending on their underlying geographic datum or method of capture. Raster data can also be represented by tabular data but is most often saved in an image specific format such as a geoTIFF or JPEG. These data can be opened in any photo viewing software but will lack the geographic information provided within a GIS or RS software. Multiple bands of data in imagery (e.g. red, green, and blue channel response as independent bands) are represented within the same image file as multiple overlapping cells. It is important to understand the metadata and file structure of each RS system a user works with as not all systems present their data with the same band numbering scheme. For example, Landsat 7, band 1 represents blue data (450 – 520 nm) whereas Landsat 8, band 1 represents coastal aerosol data (430 – 450 nm) and band 2 represents blue data. Data from different bands within an image are projected onto the exact same grid but these grids may differ between images that cover the same area at different time-points; this can become an issue with high resolution data when high spatial precision is required to compare conditions between time points. Some RS systems will deliver their data in a proprietary data format but most GIS and all RS software can convert these data to more accessible formats.

A challenge with RS data is managing, storing, and working with the relatively large files. With high spatial resolution and many bands, a single image can be over one gigabyte in size. The data are often delivered as a single image file with a geographic identifier in a separate file, but the image file itself takes up the majority of the size on disk (>98%). Many modern satellite systems will have data files exceeding one gigabyte, with a full Landsat 8 [Multi-spectral satellite with 30 m resolution (10 m panchromatic band, 100 m thermal bands), 11 bands, NIR] file requiring 1.6 GB of storage for a 3,300 square kilometer scene and Sentinel-2 [multi-spectral satellite with 10 m resolution (20 m red-edge and SWIR, 60 m water vapour band), 12 bands] requiring 500 MB of storage for a 100 square kilometer scene. Higher resolution products or hyperspectral products can easily exceed 10 GB of storage per image.

In these ways, RS data are unique from other tabular or GIS data. The power of RS data comes from their continuous nature, but that results in large file sizes and requires adequate storage space and computational power.

REMOTE SENSING SOFTWARE

While most GIS packages include some RS capabilities (e.g., image manipulation, and basic image processing/classification), true RS software provide a wider array of techniques that are generally easier to undertake, access, and customize. ESRI's ArcPro (ESRI, California, USA) has made significant strides towards becoming a more viable RS software but it is still limited when compared to other options like ENVI (Harris Geospatial, Colorado, USA) or eCognition (Trimble Geospatial, California, USA; for more RS software, see Table A4). There are also proprietary software available from some satellite image providers, which are dedicated to processing their own image data (e.g., SNAP for Sentinel data). Often a project will require the use of multiple software, which usually include a dedicated GIS software in addition to a dedicated RS software.

AVAILABLE SOFTWARE

To date, the most common RS software are ENVI (Harris Geospatial, Colorado, USA), ERDAS IMAGINE (Hexagon AB, Stockholm, Sweden), and eCognition (Trimble Geospatial, California, USA). Whereas the former two are general RS software, eCognition is primarily used for object-based image analyses where pixels are grouped according to their value and proximity (discussed in more detail in Common Remote Sensing Techniques section). The resulting data becomes vectorized and can enhance the accuracy and speed of further functions/calculations when the input data are of high spatial resolution. Other software like the SNAP Toolbox (European Space Agency) are similarly specialized; while usable on any input raster data, the tools and functions within SNAP are designed to be automated for the Sentinel series of satellites.

Most RS software have distinctive features, tools, or workflows that make certain analyses easier to perform or allow for a greater range of adjustment than other software. For example, eCognition allows for the most in-depth object-based analyses of the software listed in Table A4, while ENVI has simple graphical interfaces for computationally complex functions like cloud detection and masking. Most RS software can support vector data as well as raster data, but they may not be as efficient at processing and displaying these as GIS software. Some software also provides cloud-based analyses where performance can be enhanced via cloud computing. The increased performance power from any device must be balanced with the potential security of these services. As RS studies will often involve more than one image as input, it is important to consider the ability of the software to automate concurrent processing of several images. While some software do this easily with a graphical interface (e.g. ENVI) it is often more powerful to leverage the internal coding language of these software. Just as in ArcMap products, some functions or calculations are only available through coding and these scripts provide easily repeatable workflows that can be applied throughout a project or to novel projects. Most software now support Python scripting which is an easy language to learn and there are considerable help resources

available online for it. Despite the availability of more user-friendly graphical interfaces and more intuitive coding languages, software users still require training on how to use these software and a base-level of knowledge on RS theory in order to properly implement an RS-based project.

In contrast to many traditional GIS software, dedicated RS software fully utilize the graphical power of computers. Many desktops and laptops now come with dedicated graphical processing units (GPUs) that are better designed to handle image processing (often used heavily in video editing and gaming); these are fully utilized by modern RS software. Because RS data are large continuous sheets of data, they require more computing power to process without significant delays to the end user. When viewing data, the user will often zoom in and out and regularly move around the image; the computer is constantly loading, projecting, and reloading data during this process. For the best results, computers that will conduct RS analyses should be equipped with a discrete graphics card and at least 8 gigabytes of RAM (random access memory) to reduce lag in the software. Since zooming and panning requires constant loading of data, a computer with more RAM will be able to keep more of the image 'in memory' and reduce load times when looking across a scene. These specifications or better are becoming standard for most computers, but older systems may not be able to meet these requirements. It is therefore important to ensure the computer to be used meets the required specifications for the software that will be used, and it is prudent to try to use a computer that exceeds these specifications to ensure a better user experience.

CLOUD COMPUTATION

Cloud computing and software has recently become a more common processing method in the sciences and RS. Initially, cloud software enabled easy sharing of tools and data, but now cloud processing leverages networked servers (with much more processing power than standard desktops) to quickly solve complex issues. Cloud processing is already in use through some RS software with tools like DroneDeploy and Google Earth Engine being exclusively cloud-based platforms. Another significant advantage to these services for the user is a decrease in hard drive storage space required for large projects and intermediate files. In larger projects there will often be data created that only serves as an input into another processing step that by itself is meaningless and cloud computing software does away with the need to save these files to one's local disk. Many of these services will also host data, which will further decrease the burden on the user. Though personal computers continue advancing in speed and capacity, it is likely that some RS functions (especially for large datasets) will be best based on cloud computing software in the near future.

In the case of Google Earth Engine, all historic and current images from freely available satellite data (such as the Landsat and Sentinel series) are pre-processed and available for immediate use. Combined with increased computational power, this has allowed for

very large mapping projects over significant time scales of countries (Sidhu et al. 2018, Traganos et al. 2018, Amani et al. 2019) and even the globe (Pekel et al. 2016, Gorelick et al. 2017, Yang et al. 2019). Canada-wide wetland maps and identification of small water bodies created with consistent methodology will be invaluable for future fish habitat works (Mahdianpari et al. 2020). With cloud computing, resources can be hosted online without the need to constantly download file revisions or new products. Many RS processes and analyses can be done with only publicly available data to generate meaningful results. Within Google Earth Engine, all processes are done via coding, which is easily transferable and shareable to all other users. Cloud-based products must be assessed for security of data if the processes require confidential, private, or otherwise sensitive information to be transmitted online. The use of these platforms should be assessed by Information Technology and Security before any widespread use is adopted within the Government of Canada.

RS software offers an experience tailored for its unique data and analyses. While traditional GIS software can conduct some RS processing, they are often less intuitive to use and do not provide as many built-in functions as RS software do. RS software can also display and process data more rapidly as they are optimized for raster data. Built-in programming language functionality can allow for consistent and shareable workflows for transferring processes across geographic scales and between project teams. As RS data get increasingly high in spatial and spectral resolution, loading and processing takes longer. Cloud computing has become a way to circumvent high computational and storage cost; data can be stored online and processed without any burden on the user's computer. Future advancements in RS software and techniques will allow for easier processing by less experienced users while allowing for very complex analyses for advanced RS analysts.

PRE-PROCESSING

Most RS data will require some amount of pre-processing in order to obtain optimal results. For image data and products that are purchased, vendors will often sell forms of pre-processing software to reduce the burden on the user. Many common and open-source data (e.g. Landsat series, Sentinel series) have their own pre-processing programs or coding scripts that can be freely accessed via the web. The type of pre-processing required depends on the data type and source, techniques to be used, and repeatability required.

A common pre-processing step is georecitifcation, where image data are accurately tied to a coordinate reference datum by use of Ground Control Points (GCPs) or highly accurate GPS (such as Real Time Kinetic; RTK). While most satellite data are delivered as a georeferenced image, aerial photography, UAV image data, and point clouds are often found without geospatial data directly attached to them. Most GIS and RS

software can georectify image data with some user input (delineation of GCPs or attributing a GPS dataset tied to image/point capture). To use GCPs, the user will specify the coordinates of known locations such as control towers (often used with data covering large spatial scales) or some form of ground marker (often used for smaller projects) where coordinates are acquired with high positional accuracy GPS devices (<1 m). These must be easily distinguishable and immovable during image acquisition as these points are delineated by the user in the software. Without GCPs, the georectification is only as accurate as the available basemap plus error in plotting. Care should be taken to only use points that are relatively immutable (e.g. building corners, rock outcrops) as any change in position of these points between years will result in a compounding error. In this regard, it can be difficult to georectify natural sites from basemap data as non-rocky natural features (e.g. vegetation, water boundaries) are variable through time. It is often the case that basemap imagery will be of lower quality or resolution than that which is to be georectified so obvious features (with high contrast) and well-defined points (corners) are best suited for this technique. Whether GCPs or manual delineation is conducted, the imagery must be altered in some way to cohere with the Earth's surface. Satellite data are often available as a terrain-corrected product where changes in elevation are accounted for (as pixels are compressed and stretched along different axes). Similar processing can be done in many GIS and RS software, which can adjust for global or local accuracy (or a combination, whichever is desired). For the final step of georectification, the user can choose to change the imagery in one or more dimensions. A zero-dimensional shift is used to line up georectified images whose pixels are not aligned; this can rotate and move the image. A one-dimensional shift is most common; this can rotate, move, and rescale (increase or decrease size) of the image. With more than three control points, higher scale transformations can take place that are akin to terrain correction. These transformations are not used as often and are only necessary under specific accuracy applications.

PASSIVE DATA PRE-PROCESSING

Passive satellite imaging systems must contend with capturing data through the atmosphere, which can degrade image quality unevenly across pixels within the image data. Most satellite data come delivered as top-of-atmosphere (TOA) datasets, meaning they are calibrated to the spectral response received at the sensor (not the surface imaged, so it includes atmospheric particles). While this does offer a standardized dataset, changes in the atmosphere can limit the transferability of algorithms between image data. For studies attempting to quantify change over large temporal scales, it is best to process the data to surface reflectance (SR). This transformation will make two image datasets relatable so that common features exhibit the same spectral response regardless of atmospheric interference. This technique is especially relevant when observing spectral indices (e.g. normalized difference indices like NDVI, Tasseled Cap Transformations) over time as small changes due to atmospheric differences can create false differences in values that incorrectly assert change over time. Some imagery have

thermal bands that can assess the temperature of land and water surfaces. For these data, thermal calibration is necessary and is analogous to atmospheric correction to surface reflection for other bands.

Clouds are a problem for passive imaging systems as they can saturate (increase values of) pixels within the clouds and de-saturate (decrease values of) pixels in their shadow. Most data from satellite sensors have pre-processed algorithms in the data received that can deduce the probability of cloud and cloud shadow occurrence. More recent satellites can detect cloud types, which are useful for detecting cirrus clouds (delicate, hair-like clouds) that are more subtle but still change the spectral response of land cover. Cloud cover in imagery can be expressed as a function of the whole scene or per-pixel. When ordering satellite imagery, whole scene cloud cover is often presented as a percentage of scene covered, which can indicate the viability of an image for use in a project. Cloud cover is also calculated at the per-pixel level where each pixel is either flagged as cloudy or assigned a probability of cloud cover; these can be used directly in GIS and RS software to 'mask' or exclude pixels that are too cloudy (Figure 4).

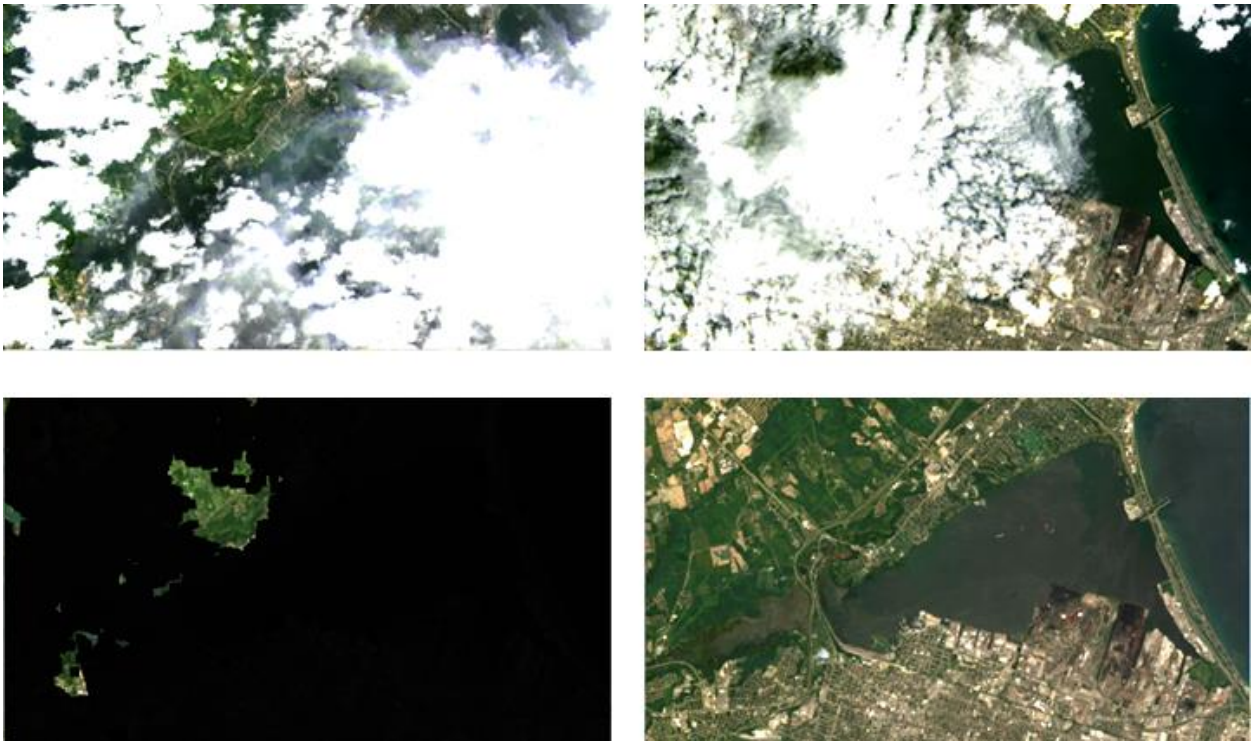

Figure 4. *Example of cloud masking. On the top row, Landsat 8 images (17 August 2019 left, 2 September 2019) are heavily compromised by cloud cover on chosen date. (Bottom left) Cloud masking eliminates all pixels contained clouds or cloud shadows to give only data uncompromised by the atmosphere for 17 August 2019 image, but removes over 80% of data. (Bottom right) Summer composite (including both top row images) of summer images with median values calculated for each pixel to eliminate cloud cover.*

ACTIVE DATA PRE-PROCESSING

The energy sent from active sensors are relatively low-powered and discrete compared to the amount of solar energy that is reflected and received by passive image sensors. Energy is sent at discrete wavelengths which vary based on the sensor used; common satellites use L-band (30 – 15 cm wavelength) and C-band (7.5 – 3.75 cm wavelength) energy. This energy will encounter unique signals and scattering that change based on dielectric (i.e. ability to absorb energy from electric fields) and surface properties (i.e. texture) of the material encountered which sends some energy back to the sensor and the majority out in other directions. As a result of these variances, these images contain speckle, which should be filtered out to increase data clarity and quality. Active systems image at non-nadir angles in order to deduce textures and geometry; changes to the imaging angle must be corrected for in pre-processing to keep the data consistent.

Due to these sensor properties, speckle is an inherent property within active RS products. As scattered waves of energy arrive at the sensor, they can be in or out of phase with each other and produce constructive or destructive interference resulting in speckle. It appears as adjacent light and dark pixels over the same land cover (Figure 5). This can affect data processing, especially with image classification, as it results in variability within land cover types that causes spectral confusion. The simplest form of speckle filtering are mean or median moving windows that look at adjacent pixels (often in a 3 x 3 or 5 x 5 square) and change the pixel to the median/mean value of these. This type of filtering is quick to conduct but treat the speckle variance as equal locally and merge the speckle into the data. More advanced speckle filtering such as the Sigma-Lee filter and Gamma-MAP filters utilize more advanced statistical techniques that look at the global and local scene together. These methods are preferable as they reduce speckle noise while preserving the inherent data (Mansourpour et al. 2006). Most speckle filtering methods use some local window analyses, which do not function properly near image borders as part of the window contains no data pixels. Data loss near image borders is therefore to be expected when removing speckle.

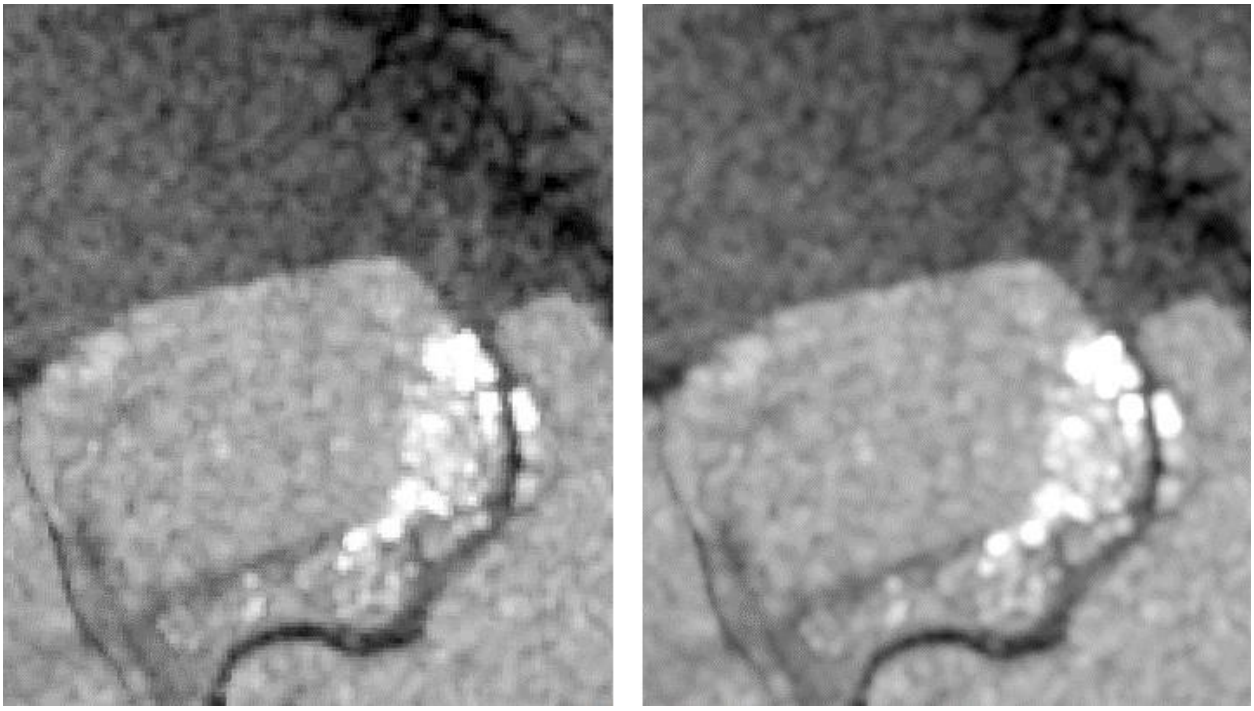

Figure 5. *Example of speckle and speckle filtering in active satellite data (Sentinel-1 HH band) in Hay River, NWT, Canada. (Left) Over a continuous land cover, the data exhibit bright and dark speckling. (Right) By using a simple mean filter over three times the input resolution (in this case, 60m), the data are 'smoothed' to reduce speckle. Note that this does decrease the spatial resolution of the image making edges (like those along the river) appear 'fuzzy'.*

As the energy received by the sensor changes relative to the distance the energy travels, imaging at an angle (e.g. 20 degrees) will produce different return values than imaging at nadir (0 degrees) over the same land cover. Images at extreme angles (>40 degrees) can exhibit slant-range distortions that can cause relief displacement (apparent change in distance from steep slopes) and terrain shadowing (data loss behind steep slopes). As they often image at non-nadir, active satellite sensors will include the imaging angle as a band, which can be used to correct for differences with various formulas (Mladenova & Jackson 2011). Since RS data are provided at large spatial scales, a difference in viewing geometry can be observed within a single scene (especially near borders) and could impact any analyses without proper corrections. Due to the above issues, it is preferable to obtain active image data with a consistent image angle, typically around 20 degrees.

When vertical changes are large and abrupt, they cause a significant difference in return values to the sensor as mentioned above. Natural terrain can be corrected for with the use of high-resolution Digital Elevation Model data to terrain-correct the image product. Depending on the angle of imaging, image shadows may also be present. Similar to shadows in true-colour imagery, active data will not be recorded on the opposing side of steep/abrupt terrain. The sides of the terrain that are 'shaded' depend on the viewing

angle and orbit of the satellite. To fully image steep/abrupt terrain, images from two or more angles/orbits must be combined.

POINT CLOUD PRE-PROCESSING

Point-cloud data can be considered a subset of active data where values are not gridded into raster format (with constant data) but come as unique vector point data. Since these data do not have consistent spacing between observed values they are not reported as pixels and instead reported as average distances (e.g. “mean 0.1 m distance between returns”). Not all energy emitted by the system will return back to the sensor due to signal scattering (due to uneven surfaces reflecting energy away from the sensor) and terrain shadows still apply with these data. Point cloud data will normally have greater return value density in areas with more consistent flat features (e.g. buildings and roads) compared to complex features (such as vegetation canopies). Like active data, there is inherent noise within the data and some form of filtering is necessary to find the true bottom.

With values that are geographically discrete, point cloud data can provide good vegetation canopy definition if the spatial resolution of the dataset is sufficient. Within vegetation canopies, some return values will be obtained from the canopy top, leaves within the canopy structure, and the actual ground. Many GIS and RS programs can delineate vegetation canopies and true bottoms by observing the spread of values over small spatial scales. The canopy top will be defined by many return values at one height (Z) and the bottom will have return values at a lower value (Z-b). Very dense vegetation (e.g. invasive *Phragmites australis*) or areas with multiple canopies (e.g. tropical forests) will have multiple bounceback signals throughout the vertical height of the vegetation. While this complicates true bottom delineation (especially with lower resolution scanning) it does make these land cover types spectrally unique. Point cloud data captured near the land-water interface requires special attention. Transmissibility of energy differs significantly between water and air, which can cause issues with point cloud data. Special underwater LiDAR sensors are available that operate within an energy range that is feasible for bottom detection in water up to a certain depth (wavelength dependent). With most other LiDAR sensors, water will cause significant signal decay and either return no data or only data from the water’s surface.

REPEATABILITY REQUIRED

Depending on the project being undertaken, pre-processing may or may not be required and different techniques used within the same project may require multiple bouts of pre-processing. In other cases, projects may require less pre-processing to conduct simpler RS methods that can yield results quickly. This is often the case for projects that require little or no repeatability; often this takes the form of basic image classification. Projects over large spatial and temporal scales need to be repeatable or automated in order to facilitate timely and consistent results. For smaller projects (focused on one area from a

single date), the additional work required for repeatable analyses over time may negatively impact the timing of deliverables. For example, if a user has one UAV image dataset from a study site and wants to classify the image into types of fish habitat, it is faster to manually delineate these classes as opposed to developing a suitable supervised image classifier. This can be even more relevant when timeliness is important such as when projects involve species-at-risk habitat or when planning field visits to specific fish habitat zones. Conversely when analyzing a time-series of images the user would want high repeatability between images to maintain a consistent end product that can be produced quickly along the entire series. In cases such as this, the initial investment in terms of time setting up a workflow is likely well worth effort since it will reduce effort later and ensure consistency throughout the project.

RS data are delivered in a usable format but should be pre-processed for many analyses. There are techniques specific to passive and active data though many are for similar purposes of equalizing data between times and scenes. While many projects should be pre-processed for repeatability, projects of small scale can omit pre-processing to hasten the results while still producing valid results.

REMOTE SENSING TECHNIQUES

A list of RS techniques can be found in Table A5. The data are split into three categories as some techniques are common between passive and active sensors and others are unique to the sensor type. In all cases, there are often specific workflows or programs designed for each sensor that take into account the sensor's design and flightpath. For example, most multi-spectral passive image sensors can conduct band arithmetic to deduce the Tasseled Cap index (Kauth and Thomas 1976) but the conversion values are specific to each sensor. It is often best to choose a sensor that is commonly used so that such calculations and applications are defined and already developed by RS engineers. Since becoming publicly available, the Landsat series and Sentinel series passive sensors have been the subject of extensive research. These have well defined processing pathways that can simplify complex analyses. Conversely, newer sensors such as high-resolution WorldView-3 are more difficult to work with but the rapid evolution of RS data and processing has led to extensive development on this sensor in just a few years (Wang et al. 2016, Kwan et al. 2017, Sibanda et al. 2017, Ye et al. 2017, Sidike et al. 2019). Some of the more commonly used techniques for working with RS imagery are presented below along with an example of how this technique has been used to support the conservation or management of natural resources.

IMAGE CLASSIFICATION

Digitization (manual classification)

The most basic method of discerning land use/land cover (LULC) within RS data is through manual classification or digitization. Using field data and expert knowledge, users will trace LULC on an image and assign them to a class (effectively vectorizing the raster data). It is best if the users have some field-level history and knowledge of the site to get the most accurate classification possible. Manual digitization can take place over a subset of the image that is not necessarily continuous (e.g. only classifying one land cover over an image, resulting in several non-touching polygons) though it is often conducted across the entire image. Care must be taken by the user to ensure that the polygon data created have suitable topology and are directly adjacent but do not overlap. The human eye and brain can interpret a significant amount of information that can sometimes exceed the abilities of computer software, especially with poor quality image data. The accuracy of the method is not generally reported and is only as good as the user, therefore experience and training can help improve classification accuracy.

Markle and Chow-Fraser (2018) manually digitized a series of historic air photos over Point Pelee National Park (Leamington, ON) to determine changes in aquatic habitat for species at risk turtles. Automated image classification was not possible due to the poor quality of the data, which were from scanned single band (black and white) film orthophotography. These data were not collected with the purpose of conducting change detection or complex RS, but the interpretive power of the user was able to extract useful information. In this study they were able to determine the changes in available habitat types throughout the park over a 40+ year time period. Manual digitizing using image-objects (discussed below) has been found to be a faster (50% time-reduction) and equally accurate as more traditional digitizing (A. Reinert, Environment and Climate Change Canada, personal communication, 2018). Manually derived image-object based classifications of images must be checked for polygon topology to ensure they do not overlap or miss areas of the image.

Supervised image classification

Image classification is an automated analysis using computer software. In supervised image classification, user input is required but the workload is significantly reduced on the human user compared to manual digitization. The user creates a set of training data for each LULC class that is determined to be present within the image and distinguishable within the dataset. It is often recommended to create 30 polygons for each LULC class, though more complex (spectrally variable) classes should have as many as feasible (Ma et al. 2015). These training data are fed into a classifier that learns the spectral profile of each LULC class and then assesses and classifies every pixel/object within the dataset. There are many classifiers that can be used in this process, with the most common ones being maximum likelihood, random forest, and

CART (Classification and Regression Trees) classifiers (Ma et al. 2017). These use different statistical methods to separate the training data classes and none are universally better or more accurate. Most RS software require the user to create training data, train a classifier, and then apply the classifier to the image data so it is relatively easy to train multiple classifiers to see which garner the best results. In order to determine the accuracy of these methods, it is common to report overall accuracy and user's and producer's accuracy of the most relevant LULC classes. To establish these measures of accuracy, an additional validation or testing dataset must be created; this is done in a similar manner to the creation of training data but is held back from input into the classifier during the training phase. The validation data will form the basis of all accuracy analyses, with an error (or confusion) matrix that describes the user's and producer's accuracy for every single class used within the analyses.

Bourgeau-Chavez et al. (2015) used a multi-sensor, multi-date image stack (one file that contains data from multiple overlapping images; in this case Landsat data combined with PALSAR data) to create an extensive LULC map of the Great Lakes shoreline that could discern unique wetland types (such as open marsh, swamp, and *Phragmites*). They used a random forest classifier with unique training and validation data for each individual stack to increase the accuracy of the classification. The error matrices were amalgamated on a lake-by-lake basis to provide a lake specific measure of classification accuracy for each LULC type.

Object-oriented image classification

A subset of image classification, an object-oriented approach is typically used with high spatial resolution datasets. While many RS software can conduct object-oriented image classification, the most dedicated and advanced solution comes through eCognition (Trimble Geospatial, California, USA). The unique feature of these analyses is image segmentation which creates polygons out of the image pixels by grouping like pixels together and separating unlike pixels (Figure 6). Most software will allow for the user to specify how these objects are created by defining the importance of inter- and intra-class values, size, and shape. These rules can be applied at multiple instances to create classification 'trees'; as an example, water is often found in large, homogenously dark patches and a specific ruleset could be used to easily classify water before classifying the rest of the image. Since high resolution data have many small pixels, there are often strong edge effects where two LULC classes will overlap and produce a mixed signal to the sensor. These data would be incorrectly classified as being from neither of their original classes in pixel-based classification. Object-oriented image classification can group like-pixels and include some mixed-pixels or 'off-values' so that tiny 'sliver' polygons are not created as they are highly unlikely to exist in reality. As per other forms of image classification, these processes can be saved and replicated across multiple images to speed up processing and decrease the burden on the user when working across multiple sites.

Object-oriented image classification can considerably reduce the burden on the user as 'polygons' are automatically created. These can be classified in an automated fashion (through an image classification scheme, as in the above section) or by manually defining each polygon (see above). Midwood and Chow-Fraser (2010) used object-oriented classification to map wetland vegetation (e.g., meadow, emergent and floating vegetation) and rock features in coastal wetlands in Georgian Bay, Ontario to quantify the area of fish habitat in each wetland. This same approach was then applied to imagery that was captured six years later to quantify the changes in vegetation cover that occurred in the intervening years when water levels were historically low and to link these changes in habitat conditions with a reduction in the diversity of fishes and change in community assemblage in these wetlands (Midwood et al. 2012).

Unsupervised image classification

Fully automated image classification requires little to no input by the user and returns a classified image without labels (i.e., the user must determine what each class is mapping on the ground). This technique is typically less accurate for full image classification and is often used as an intermediate step within another form of image classification (e.g., unsupervised classification is applied to an image to find general groupings and then a supervised classification is applied only to general groupings of interest). Common unsupervised classifiers include k-means, ISO clustering, and X means. Some require the user to set the number of classes to be created while others will determine the most feasible number of distinguishable classes from within a given range. As with supervised classifiers, unsupervised classifiers will separate the data into the most distant (or most separated, on a graph) classes but do so without knowledge of what they are separating or where to start separating from. The resulting classification appears the same as supervised classification but does not contain meaningful class labels; the user will later define the classes manually.

Sobiech and Dierking (2013) used an unsupervised classifier to delineate lake ice with SAR (synthetic aperture radar) image data. Water absorbs almost all incoming energy and thus has extremely low return values at the sensor, whereas ice (and snow) has much higher returns. By using a k-means classifier, Sobiech and Dierking (2013) were able to automatically separate the image of a waterbody into water (one class) and ice/snow (one class) quickly with minimal input. While the classification itself does not indicate if the class is ice or snow, it isolates these areas of interest so that additional classification methods can be applied that are focused solely on distinguishing ice and snow.

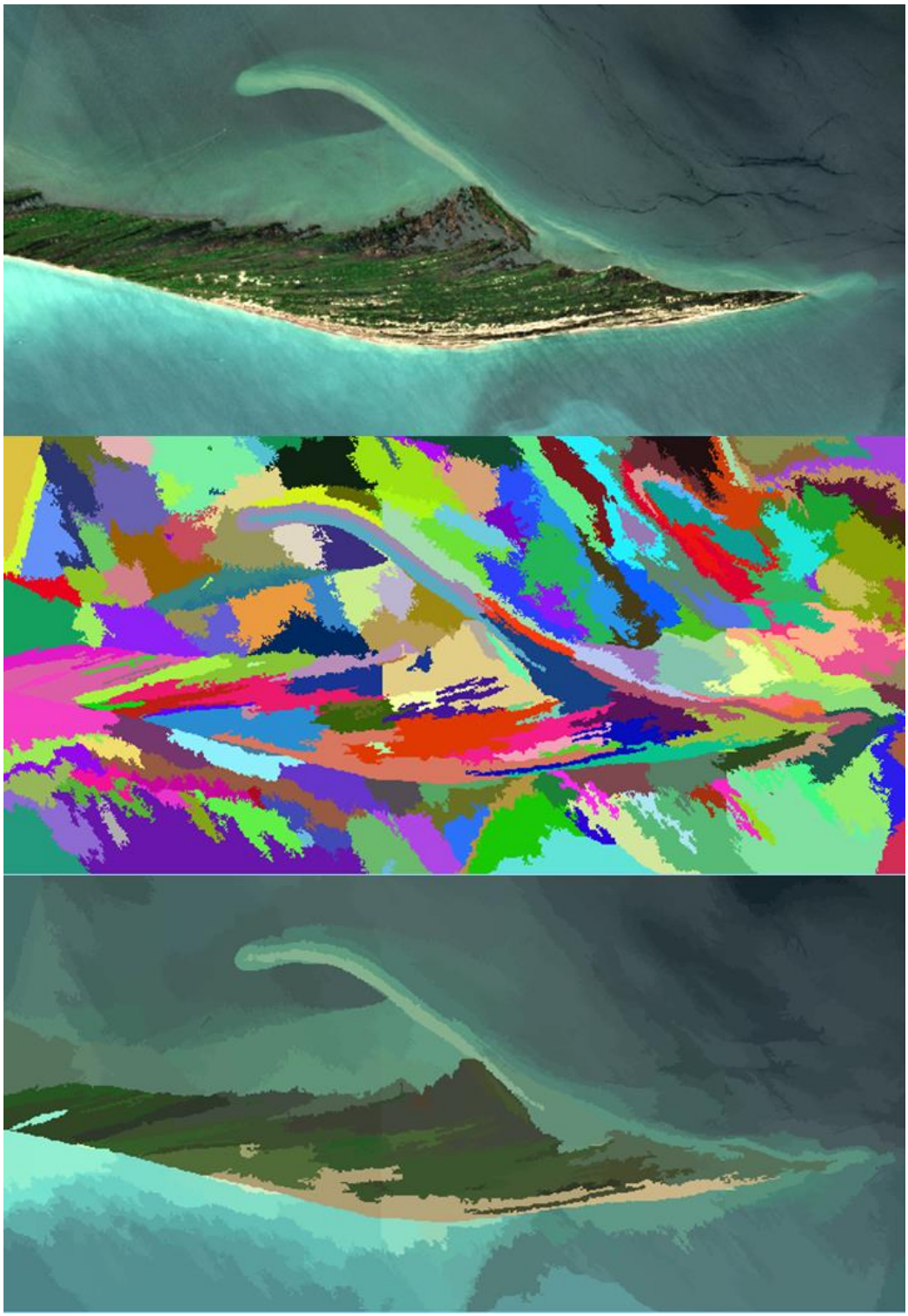

Figure 6. *(Top) A Sentinel-2 visible spectrum image (red, green, and blue bands) from June 2019 over Long Point, Ontario; (Middle); the same image after image object creation, with unique objects shown in random colours; (Bottom) the same image objects of Long Point classified according to mean value in all spectral bands.*

Artificial Intelligence and Deep Learning in image classification

The further development of Artificial Intelligence (AI) programs will have a significant impact on image processing and RS software. Machine Learning has been the focus of most RS research in the past, most commonly with Maximum Likelihood, Random Forest, and Support Vector Machine (Maxwell et. al 2018). These processes require fine tuning inputs (e.g. labelled training data, parameters) in order to obtain good results. In contrast, Deep Learning (DL) and Neural Networks (NN) need few inputs but require large amounts of training data and computing power to handle them. DL and NN take the input data and create many connected 'learned' processes that lead to unique outputs. These processes take a 'black box' approach in that the internal learning structure of the model is not known or specified but this allows for the reduced inputs in DL and NN (compared to Machine Learning). Common toolkits used in RS to conduct these processes include TensorFlow, Keras, and PyTorch; these are often accessed through coding (e.g. Python, R) and have options to conduct processing on a cloud server to reduce computational demands on local machines. Development of NN and DL has made significant advances towards fully automated image classification with complex data and LULC. van Duynhoven and Dragićević (2019) showcase the capacity for AI in analyzing changes in land cover and reporting higher accuracies with limited input data (similar results were also found by Kwan et al. 2020, Ayhan and Kwan 2020, and Miyoshi et al. 2020). With ever-increasing image data and classifications to draw from, software like Pix4D has been able to automatically classify some classes within images (e.g. forest, road, building) without any input by the user. In the future, it is likely that broad, simpler classes (e.g. forest, roads, water) could be automatically generated with advanced AI systems using repositories of existing classifications. This will ease the computational burden on the user but will still require advanced RS users to complete full, detailed classification of images. As future research proceeds with AI in RS, the ease of use and development within current RS software will continue to expand and become more commonplace within the field.

CHANGE DETECTION

One of the most common techniques in RS is change detection. Change detection is a comparison of two or more data sets in the same geographic area but at different time points. This can be conducted with varying degrees of complexity depending on the needs of the project. At the very basic level, change detection can be conducted visually between two images of the same scene (even two images without the same viewing angle). The user simply compares the features of interest between the two images to identify differences or changes in the images. Most data currently used in RS will have consistent image properties that allow for more complex analyses to take place. Generally, some method of image classification (manual, unsupervised, or supervised) is applied to each image of interest and the shift in LULCs (Land-use, land-cover, e.g. forest, water, urban area, vineyard) between dates can be defined (i.e., change in LULC

type) and quantified (i.e., LULC type expands or contracts). Most GIS and RS software have some functionality to allow users to easily (or automatically) conduct these analyses and visualize the changes within their dataset.

Jung et al. (2017) used manual digitization to discern changes in wetland vegetation composition over a 30-year timescale. This allowed them to document the invasion of non-native common reed (*Phragmites australis* subsp. *australis*) throughout Long Point National Wildlife Area, which included the identification of new patches of *Phragmites* as well as the rates of expansion outward from established patches. The manually digitized maps were further used to develop a predictive model to identify areas where *Phragmites* was likely to expand into, which supported an assessment of risk from *Phragmites* invasion for critical habitat for species at risk.

DATA FUSION (BY DATE OR SENSOR)

Some LULCs are indistinguishable for a given sensor at a particular point in time, but they may be easily separated by other RS platforms or at other dates. Advanced computational power has allowed for data fusion, a common technique to stack data from multiple sensors and dates into one large image. Classifications can then be developed that use a variety of characteristics of a LULC type to arrive at a final class type for pixel. This approach is best explained through examples of how it can be used. When conducting these analyses, care must be taken to ensure consistent pre-processing for the stacked image data. If the image alignment or pre-processing differs within a stack it will cause significant issues with any analyses.

Bourgeau-Chavez et al. (2013) found that passive image data from Landsat could distinguish wetland classes from other LULCs but could not differentiate within wetland classes. They combined their passive data with active PALSAR (L-band SAR) data in order to increase discernibility among wetland classes. Combining images from multiple dates (i.e. spring, summer, and fall) helped to further distinguish wetland vegetation due to their phenological differences at these times. While *Phragmites* and *Typha* spp. are similarly green and dense in summer, the former stands taller in spring imagery and have unique purple fronds (from seeds) in later summer/fall images.

PASSIVE-SPECIFIC REMOTE SENSING TECHNIQUES AND EXAMPLES

SPECTRAL POWER DISTRIBUTION

In order to specify a LULC class, the user will most often use field-based observations to ensure the validity of their classification (as described above). With the use of a spectroradiometer, the user can assess the spectral power distribution of a LULC class to determine the exact reflectance across a large spectrum of electromagnetic energy. Using this approach, spectral profiles are created that represent the reflectance of these

LULCs as they would be seen from the sensor (aerial- or satellite-base) being used in the study. This approach requires specialized and expensive instrumentation but provides a means of better differentiating LULC classes of interest. If suitable for a project, spectral profiles can be used to automatically assign pixels/objects to a LULC class or determine the likelihood that it is part of this specific class. This can be a powerful tool for species delineation with high resolution imagery or for any project where there can be high spectral confusion among LULCs.

Brooks et al. (2019) used this technique to determine the spectral profile of invasive Eurasian water milfoil (*Myriophyllum spicatum*) in the Great Lakes. By also conducting these analyses on other submerged aquatic vegetation (SAV), they were able to determine the spectra required in a sensor in order to accurately discern Eurasian water milfoil from other species. Since these species of SAV are found within the water column, Brooks et al. (2019) took measurements of the plants both out of the water as well as in the water (with the field spectroradiometer held just above the surface of the water). This approach can help to determine the feasibility of class distinctions for a range of sensors and in this study, Eurasian water milfoil was found to not be distinguishable from other aquatic vegetation for most common sensors.

BAND RATIOS/ARITHMETIC

The data derived from RS platforms comes as a numeric representation of reflectance for a particular wavelength or bands of electromagnetic energy. While each band of data offers a distinct view of planetary surface properties, these bands can be combined in a mathematical formula to leverage different reflectance properties of LULC classes among wavelengths. One of the most common approaches is the application of band ratios, such as:

$$\frac{(B1 - B2)}{(B1 + B2)}$$

Where B1 and B2 are two bands representing reflectance in different wavelengths.

In RS these are referred to as normalized difference (ND) ratios. There are many ratios that have been developed, including those for vegetation (NDVI; vegetation index), snow (NDSI; snow index) and moisture (NDMI; moisture index). There can also be more complex mathematical equations applied to the input bands, such as the Enhanced Vegetation Index, which uses Near-infrared (NIR) and Red bands but adds a Blue band term or the Tasseled Cap transformation (Kauth and Thomas 1976). Many RS indices make use of bands derived from Landsat satellites as these have the longest continuous dataset; for example, the NDVI uses NIR and Red bands as defined by Landsat (0.845–0.885 µm for NIR, 0.63–0.68 µm for Red). Many of the simpler methods are applicable across other sensors with similar spectral properties (e.g. NDVI works with Sentinel-2 data even though the wavelengths for NIR and Red are slightly

different), but more complex models are sensor specific (e.g. Tasseled Cap coefficients must be determined for each individual sensor). Using these band ratio or arithmetic techniques, the user can increase the number of input values for LULC classification, which increases the usability of the dataset and the differentiation of certain land cover classes. Only the computations necessary for the project should be undertaken as more complex arithmetic (e.g. Tasseled Cap transformation) require significant computational power and will increase the size of the dataset as additional bands are added.

Shuchman et al. (2013) describe a formula for depth-invariant aquatic vegetation mapping. While submerged aquatic vegetation can be detected by human observers in some satellite data, it is difficult for computer systems to consistently delineate this LULC across different water depths. As light penetrates deeper into the water column, the reflectance value of the substrate and vegetation change dramatically due to attenuation and scatter, this can cause confusion during image classification since reflectance values will differ for the same LULC based on depth. Using submerged aquatic vegetation as a training class separate from water is not suitable if the depth of water within the image varies greatly; deep areas can be mistaken as vegetation or only vegetation within a certain depth range will be delineated. Shuchman et al. (2013) developed the Submerged Aquatic Vegetation Mapping Algorithm (SAVMA) which uses deep water (where no bottom reflectance is visible) and shallow water (where bottom is reflected) to create a linear equation to correct for the effects of water on the observed reflectance. This technique is easily determined from RS data alone and does not require extraneous field data or knowledge of any water quality parameters of the water body being observed (common among other similar techniques). Since the effect of water can be effectively ‘removed’ by applying the linear equation to relevant bands (i.e. higher energy wavelengths that penetrate the water column), bottom type can be mapped to the observable depth within the image’s and water body’s specifications. SAVMA was applied over several areas in Lake Michigan and Lake Ontario to demonstrate the applicability of this algorithm. Using this in a time series, they determined that the maximum observable depth changed as a function of water quality parameters within Lake Michigan but still provided enough information to map sandy substrates and submerged aquatic vegetation in low or high densities.

AERIAL PHOTOGRAPHY

While satellite imagery has become the standard for RS information since the advent of consistent high-quality data, aerial photography has been used for many decades before the first satellites were launched into orbit. Aerial photography can still be a useful technique today as it can obtain high resolution data (usually less than 50 cm/pixel) that does not have significant atmospheric effects since the sensor is much closer to the observed surface. Many systems are available today, including those that integrate both passive RS systems with active LiDAR systems. Many of these systems include high accuracy GPS, though this is a relatively modern addition. Most flight plans

for orthophotography will fly low in altitude (2,000 to 5,000 m) and at low speed in order to obtain good quality imagery at nadir with sufficient overlap between images. Without overlap, it is difficult to stitch individual image frames together to create a seamless map unless good quality GPS data are available for each scene. Since the sensor is close to the observed surface, each image does not cover a large area and must be stitched together to form a cohesive map. The completed “product” for an area of interest is often many ‘tiles’ of image data that form a single map. These acquisitions are conducted exclusively for the needs of the purveyor and as such orthophotography will often only include relatively small geographic areas. An exception to this would be provincial and national efforts for mapping such as the Ontario Orthophotography Projects, which aim to map the southern half of the province with high resolution aerial imagery every five years.

While there are historical datasets for airphoto (many from war efforts in the early to mid 1900s), they were often not captured with orthophotography in mind, rather they were used for reconnaissance. An example of this can be found from imagery and mapping from World War II: extensive collections are available, but the imagery are often of singular locations at oblique angles and do not represent consistent nadir acquisitions with sufficient overlap in parallel rows. This makes the imagery difficult or impossible to use with many modern RS techniques, though they can be used for simple visual observation (as was their intended purpose).

Marcaccio and Chow-Fraser (2018) mapped invasive *Phragmites* throughout roadside habitat in southwestern Ontario using images collected as part of the Southwestern Ontario Orthophotography Project. These data are high resolution (30 cm resolution) but are only acquired once every five years, with the first year only capturing data in the visible spectrum (2006) and subsequent collections also obtaining NIR band data. These data were of sufficient resolution for monitoring the invasion of *Phragmites* as small patches from one image collection (<5 m2) can quickly expand to large conglomerated patches, which are difficult to eradicate (Marcaccio and Chow-Fraser 2018). The long time-gaps between acquisitions are not ideal for invasive species monitoring (i.e., to facilitate annual eradication efforts for *Phragmites*), but these data did serve as a good regional/provincial dataset to map large-scale changes and demonstrated the utility of these high-resolution images for mapping *Phragmites*.

UAV IMAGERY

Similar to orthophotography, Unmanned Aerial Vehicle (UAV) imagery is collected at the discretion of the user and is flown in close proximity to the surface. The main difference is the use of unmanned aerial/autonomous vehicles to obtain the imagery (as the name implies). Advantages of UAVs are that they can capture higher resolution imagery than aircraft since they are much closer to the ground (<100 m) and they are easier to deploy. These systems cannot cover the same spatial area as plane or helicopter-based

systems during a single flight since they are restricted by the life of their onboard batteries. Since the UAV system is a one-time purchase, these can be used to consistently map an area on a small timescale (daily or less) without incurring significant additional costs. As with orthophotography individual images must be stitched into a final map, which requires specialized software (e.g. Pix4D, Agisoft; see Table A4).

Marcaccio et al. (2016) used UAV imagery to determine the extent of invasive *Phragmites* in a coastal wetland on Lake Erie. While orthophotography data were captured over this area, the timing was not adequate for delineation of *Phragmites* and other wetland species. Available satellite data were too coarse to distinguish small patches of *Phragmites*, which are vital to map for restoration purposes. With a UAV, Marcaccio et al. (2016) obtained <10 cm resolution image data of the field site and the resultant data were better than other imagery products at identifying wetland plant types based on field verification data. Multiple sensor types exist for UAVs and can be interchanged on some systems which places the burden of knowledge on the purchaser of these systems. Regardless of band choice for passive systems, sensors that can be easily calibrated to solar irradiance will provide standardized reflectance across imaging times and dates that make comparisons easier to conduct. The authors determined an ideal RS workflow to effectively map and monitor invasive *Phragmites* within coastal wetlands, which included the use of UAVs on a site level basis. The areal limitations of UAVs restrict them to these smaller scales, but the ability for rapid and repeated imaging makes them an integral source of a RS program for invasive species.

STEREOSCOPY AND STRUCE-FROM-MOTION

With sufficient overlap (approximately 70%) between them, images collected from airborne or satellite platforms can be stitched together to form a two-dimensional map. Between each image capture, the sensor will have moved, which provides a slightly different viewing angle of the same objects (when there is appropriate image overlap). This means that between one image and the next, one object will appear in a slightly different location if it is at a different location on the z-axis (vertical axis) when not observed at nadir. This is analogous to observing tall objects (such as trees or skyscrapers) straight up from ground level: tall objects close to you appear to rise straight up, whereas tall objects further away from you appear to lean or move in multiple planes. The relative difference in location between images of these objects represents their height, and if sufficient overlap is obtained between images a 3D point cloud can be created from them. Historically this was done by using a stereoscope, where each eye would look at a different image to create the perception of depth. Modern RS software can create and analyze these point clouds and determine a z-axis value for points within the image through a process called ‘Structure-from-Motion' (Figure 7). While similar to active data methods like LiDAR, image stereoscopy is limited to the observed points of an image, which means that this approach cannot accurately determine canopy-ground differences. In addition, each point used for these analyses

must be uniquely identifiable between the two images; while computer processing and computer vision capabilities have increased greatly in recent years, this can still be a limiting factor especially with surfaces or objects that are homogeneous (e.g. flat water) or complex (e.g. dense grasslands). Stereoscopy should not be viewed as a substitute for dedicated DEM/DSM products (e.g., LiDAR), but it can provide similar (but lower quality) data with sufficient image overlap.

Husson et al. (2017) used stereoscopy-based ‘Structure-from-Motion' with UAV data in Lake Osstrasket in northern Sweden. To obtain sufficiently high resolution and overlap, a flight height of 150 m was used (creating a 5.6cm pixel) and image overlap was set to 70% both vertically and horizontally. Agisoft Photoscan (Agisoft LLC, St. Petersburg, Russia) was used to create a digital surface model (DSM); these data were added as an additional band to the visible-spectrum image data. Using an object-oriented approach, image classification accuracy for the non-submerged wetland plants was significantly higher in every case when the DSM data were included in the classification tree. Since most aerial photography and UAV projects can easily generate surface height data, this should be a common technique within a remote sensing workflow with these data. While satellite data do not often have sufficient overlap in close temporal proximity to conduct ‘Structure-from-Motion' analyses, similar analyses could be conducted with surface height data from another source (e.g. world DEM from 90 cm TanDEM-X).

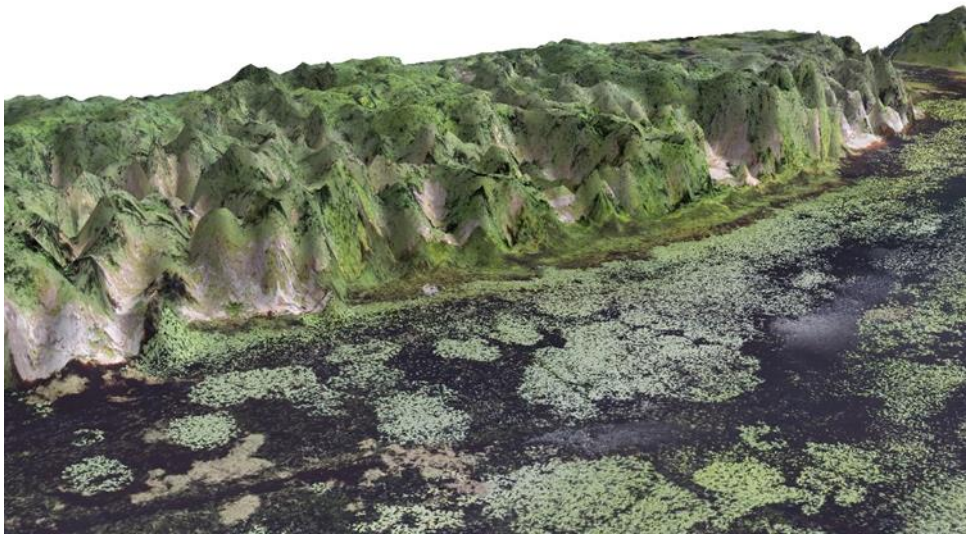

Figure 7. *Three-dimensional terrain view of a coastal wetland in Lake Huron constructed via stereoscopy/SFM from a UAV. Verticality has been exaggerated by five times to better demonstrate the range of height values available. The constructed DSM is shown with visible spectrum data overlain but can also be utilized separately.*

ACTIVE REMOTE SENSING TECHNIQUES AND EXAMPLES

INTERFEROMETRIC SAR

Since active RS sensors send out a consistent amount of energy, small changes in the response to the sensor over short time periods can only be due to changes in the surface. Interferometric SAR, or inSAR, looks for small changes in the spectral response, which can detect even millimeter changes in the surface imaged. Two SAR images covering the same geography within a small time period (from a dual-sensor satellite or multiple replica satellites flying in tandem) from slightly different view angles must be co-registered so that each pixel represents the same geometry on the imaged surface. After cross-multiplication of the images the difference or phase signal is calculated. These can be used for DEM generation but also geometry deformations from natural disasters (earthquakes, landslides), glacial and ice flows, and volcanic activity. While this technique is intensive to process and requires dedicated imaging (due to the timescale restrictions) it is very powerful for detecting small changes to the geometry of the Earth's surface.

inSAR can take advantage of a system's specific wavelength and polarizations to create interferograms that are sensitive to unique land cover types. C-band SAR, like RADARSAT has unique responses to water and vegetation in the HH (horizontal send, horizontal receive) polarization, which Brisco et al. (2017) leveraged to conduct water level monitoring in wetlands. Even with relatively long intervals between repeat images (average 24 days) wetland water levels could be accurately determined. They were also able to delineate treed and shrub wetlands throughout the image, which are notoriously difficult to identify in standard optical/passive imagery. This approach cannot, however, be applied to open water bodies that are likely to experience wind and wave action, since wind-driven changes in surface elevation will likely be greater than short-term changes in water level.

POLARIMETRIC DECOMPISITION

Active RS platforms rely on microwave-scale energy to image and this type of energy is sensitive to the texture of LULC. Textured surfaces will uniquely reflect incoming energy and can be classified into four types. Smooth surfaces like roads and calm water exhibit surface scatter where all energy bounces off the surface together without a polarization phase shift. Double-bounce is obtained when there are corners or angles in a surface (such as wall/ground interfaces) where energy strikes a surface twice before returning to the sensor; in this way the energy can be angled away from the sensor and undergo a phase shift resulting in a different signature than if it were flat. When there are multiple obstructions that the energy encounters it is deemed volume scattering; vegetation is a common LULC type that causes this. Volume scattering can cause the sensor to record many unique values for a single LULC as the energy may return at different distances, phases, and angles. A unique type of double bounce/volume scattering is called Bragg

scattering and is the result of a surface containing a wave pattern of a distance that is within the range of the energy wavelength being emitted by the platform. In RS Bragg scattering is typically confined to instances of waves on water bodies, which can cause significant constructive interference and increase the energy signal detected by the sensor. To make these details easier to ascertain by RS analysts, spectral decomposition can be performed, which creates a new band of information for each scattering mechanism; the most common of these techniques are the Freeman-Durden and Cloude/Pottier decompositions (Freeman and Druden 1998, Cloude and Pottier 1997).

Wetlands are comprised of many different species of vegetation, which can make image classification difficult based solely on spectral properties. With so much variability, simply classifying land cover as broadly 'wetland' can lead to confusion with other classes. Polarimetric analyses of plant species can help make delineation of these classes easier for the user. Atwood et al. (2020) examined the properties of *Typha* dominated wetlands, which are common throughout Canada. Since these are tall, freestanding species, they exhibit an abundance of double bounce and volume bounceback as the emitted energy gets caught in their dense canopies. While the authors found modelling these structures from mathematical models possible, there were significant seasonal changes that led to unexplained variations found in RADARSAT-2 data.

POLARIMETRIC ANALYSIS

Dielectric properties, which are determined from the chemical structure of the material and how it responds to electric polarization, vary among LULC and can affect active RS sensors. Conductive materials like metals and salt water will have a greater response back to the sensor than insulated materials like fresh water and wood (regardless of texture). Studying the dielectric properties of materials in active RS is useful for polarimetric analyses, which can help to automate image classification (similar to spectral power distributions with passive RS). While some LULC can be very complex, basic and consistent land cover types like open water and concrete can be separated by their dielectric properties.

Polarimetric analyses have been conducted on ocean and lake ice, as observing and classifying sea ice is of interest for shipping and Arctic marine travel. Surdu et al. (2015) successfully used RADARSAT-2 data to identify ice formation and break up in shallow Alaskan lakes. While RADARSAT-2 does not offer frequent repeat cycles (i.e., it does not pass over the same area of interest on a regular basis), Surdu et al. (2015) found that ice-on and ice-off could be accurately modelled when compared to the Canadian Lake Ice Model. Muhammad et al. (2016) similarly showed that lower spatial resolution MODIS data could be used to monitor these same outputs within the Mackenzie River with the advantage of daily image acquisition.

DEM/DTM GENERATION

Both Digital Elevation Models (DEM; bare-earth) and Digital Terrain Models (DTM; covered earth) can be generated from active RS data. Since these data use known energy values that are tracked from emission to reception, they can generate accurate and high-resolution (roughly two times ground resolution) changes in elevation on a surface. Passive data can also produce DTMs but they are generally lower resolution than the dataset (often 2 – 5 times) and do not penetrate canopies well. In contrast, active data creates a high-resolution product and can distinguish canopies and hard bottoms, though this varies depending on the spatial resolution and wavelength used. For satellite data, DEMs and DTMs are created using inSAR techniques (see above) and rely on gridded raster data. These will often use satellites with two opposite look sensors (e.g. TanDEM-X) placed on an angle to reduce 'land shadows'. When steep terrain is encountered, a single look system will not be able to capture data on the trailing or 'cliff' edge leading to a 'land shadow' effect. While an off-nadir angle is required to produce good DEM data, it can lead to a more pronounced shadow if two opposite look angles are not used. Good data can also be obtained by a single sensor that passes the same location with a different view angle or direction of travel within a relatively short time span.

The Government of Canada maintains a database of high resolution DEMs and DTMs generated by LiDAR known as the High-Resolution Digital Elevation Model (HRDEM). In early 2020, an updated version of the ArcticDEM was released that covers all the territories at 5 m resolution. While not a contiguous product for the rest of the country, it does cover many areas of higher population density and is generally available at a higher 1 m resolution. The dataset is available from: https://ftp.maps.canada.ca/pub/elevation/dem_mne/highresolution_hauteresolution/. LaRocque et al. (2020) used these data as valuable input into their wetland mapping project in southern New Brunswick. They took these raw data values and created other topographic metrics such as slope, profile and plan curvature (convergence and divergence of flow across a surface), topographic position index (a measure of elevation relative to surrounding pixels), and topographic wetness index (a measure of area and slope draining into a pixel). Along with optical and active satellite data, they were able to map 11 distinct wetland classes at a very high accuracy over 95%. While the most important variable for wetland delineation was the DTM, the topographic wetness index and topographic position index were also valuable contributors to the model. This was an excellent example to show that non-optical data can significantly contribute to image classification in wetland systems.

POINT CLOUDS

Most point cloud data (e.g., aircraft, UAV, or handheld) will generate point clouds that are viewed as vector data (e.g., points in space) instead of raster. The systems are often quoted with a precision (akin to pixel size) and viable distance (since the sensor is limited in power due to design constraints and health restrictions). These are most often used for DEM/DTM generation, but recent advances have led to the development of more wavelengths for unique land cover mapping (like species-specific mapping) and multiple wavelength systems for multi-surface mapping (such as combined land/water DEMs). The ground resolution of these sensors is highly dependent on the distance to the surface and speed of the sensor, although most systems will come with a specific recommendation to achieve optimal results. LiDAR (Light Detection and Ranging) technology is the most known form of point cloud data; these can generate especially high-resolution datasets over small- to medium-spatial scales.

Vernal pools and small wetlands can be especially difficult to map given their cryptic nature and seasonality. In order to capture these small wetlands, Riley et al. (2017) used a lidar-based DEM over Wakulla County, Florida with 1.52 m resolution and 8.6 cm root mean square error vertical accuracy. Using a topographic position index, Riley et al. (2017) were able to identify wetlands and vernal pools given small depressions in the elevation profile. They were also able to identify pools based on their ponded duration, though longer duration or permanent pools were more accurately classified than shorter duration pools. It would be nearly impossible to identify these depressions using lower resolution datasets that are often derived from satellite data. The methods presented in Riley et al. (2017) do have higher rates of commission than omission, though the former is preferable when dealing with such inscrutable wetlands.

CONCLUSIONS

RS provides tools and data that can streamline current analyses and open a new line of research and questions to be addressed. RS provides users the ability to provide continuous data over large spatial scales, which are not addressed through field work or other GIS work. Tools in RS software such as image classification and DEM generation can provide additional, high quality data for other analyses within RS, GIS, and other software. While many operations within FFHPP are currently conducted with some RS (e.g. basic visual identification), incorporating further skills and support with advanced RS analyses could drastically improve the speed and quality of the data being used and generated. With satellite data, there are long (>30 year) historic datasets available; long-term datasets can provide continuous spatial analysis of climate change, habitat transitions, and human alteration. Further advances in computing and cloud power will more easily provide larger (spatial and temporal) scale analyses and potentially automate some basic RS tasks. RS will provide a significant benefit to the overall

freshwater fish habitat management program through its own work and collaborations with current GIS, statistical, and field-based analyses.

ACKNOWLEDGEMENTS

The authors would like to thank Carolyn Bakelaar, Andrew Doolittle, Maja Cvetkovic, Sheeva Nakhaie, Stuart Campbell, and Chris Biberhofer for their input and recommendations for the necessary scope and details of this document. We are also grateful for the constructive feedback two peer-reviewers. Funding for this project came from the Freshwater Habitat Initiative of Fisheries and Oceans Canada.

REFERENCES

Amani, M., Mahdavi, S., Afshar, M., Brisco, B., Huang, W., Mohammad Javad Mirzadeh, S., White, L., Banks, S., Montgomery, J., & Hopkinson, C. 2019. Canadian wetland inventory using Google Earth Engine: The first map and preliminary results. Remote Sensing, 11(7): 842. doi:10.3390/rs11070842

Atwood, D., Battaglia, M., Bourgeau-Chavez, L., Ahern, F., Murnaghan, K., & Brisco, B. 2020. Exploring polarimetric phase of microwave backscatter from Typha wetlands. Canadian Journal of Remote Sensing, 46(1): 49–66. doi:10.1080/07038992.2020.1726736

Ayhan, B., & Kwan, C. 2020. Tree, shrub, and grass classification using only RGB images. Remote Sensing, 12(8): 1333. https://doi.org/10.3390/RS12081333

Bourgeau-Chavez, L. L., Kowalski, K. P., Carlson, M. L., Scarbrough, K. A., Powell, R. B., Brooks, C. N., Huberty, B., Jenkins, L.K., Banda, E.C., Galbraith, D.M., Laubach, Z.M., & Riordan, K. 2013. Mapping invasive Phragmites australis in the coastal Great Lakes with ALOS PALSAR satellite imagery for decision support. Journal of Great Lakes Research, 39(S1): 65–77. doi:10.1016/j.jglr.2012.11.001

Bourgeau-Chavez, L., Endres, S., Battaglia, M., Miller, M. E. M., Banda, E., Laubach, Z., Higman, P., Chow-Fraser, P., & Marcaccio, J. 2015. Development of a bi-national Great Lakes coastal wetland and land use map using three season PALSAR and Landsat imagery. Remote Sensing, 7(7): 8655–8682. doi:10.3390/rs70708655

Brisco, B., Ahern, F., Murnaghan, K., White, L., Canisus, F., & Lancaster, P. 2017. Seasonal change in wetland coherence as an aid to wetland monitoring. Remote Sensing, 9(2): 158. doi:10.3390/rs9020158

Brooks, C. N., Grimm, A. G., Marcarelli, A. M., & Dobson, R. J. 2019. Multiscale collection and analysis of submerged aquatic vegetation spectral profiles for

Eurasian watermilfoil detection. Journal of Applied Remote Sensing, 13(3): 037501. doi:10.1117/1.JRS.13.037501

Cloude, S. R., & Pottier, E. 1997. An entropy based classification scheme for land applications of polarimetric SAR. IEEE Transactions on Geoscience and Remote Sensing, 35(1): 68–78. doi:10.1109/36.551935

Dauwalter, D.C., Fesenmyer, K.A., Bjork, R., Leasure, D.R. and Wenger, S.J. 2017. Satellite and airborne remote sensing applications for freshwater fisheries. Fisheries, 42(10): 526-537. doi:10.1080/03632415.2017.1357911

Freeman, A., & Durden, S. 1998. A three-component scattering model for polarimetric SAR data. IEEE Transcations on Geoscience and Remote Sensing, 36(3): 963–973.

Gorelick, N., Hancher, M., Dixon, M., Ilyushchenko, S., Thau, D., & Moore, R. 2017. Google Earth Engine: Planetary-scale geospatial analysis for everyone. Remote Sensing of Environment, 202: 18–27. doi:10.1016/j.rse.2017.06.031

Government of Canada. 2012. Pathways of Effects National Guidelines. Fisheries and Oceans Canada. 32 pp.

Hugue, F., Lapointe, M., Eaton, B. C., & Lepoutre, A. 2016. Satellite-based remote sensing of running water habitats at large riverscape scales: Tools to analyze habitat heterogeneity for river ecosystem management. Geomorphology, 253: 353–369. doi:10.1016/j.geomorph.2015.10.025

Husson, E., Reese, H., & Ecke, F. 2017. Combining spectral data and a DSM from UAS-images for improved classification of non-submerged aquatic vegetation. Remote Sensing, 9(3): 247. doi:10.3390/rs9030247

Jung, J. A., Rokitnicki-Wojcik, D., & Midwood, J. D. 2017. Characterizing past and modelling future spread of Phragmites australis ssp. australis at Long Point Peninsula, Ontario, Canada. Wetlands, 37(5) : 961-973. doi:10.1007/s13157-017-0931-3

Kauth, R. J. and Thomas, G. S. 1976. The Tasselled Cap -- A Graphic Description of the Spectral-Temporal Development of Agricultural Crops as Seen by LANDSAT. LARS Symposia. Paper 159. Available from: http://docs.lib.purdue.edu/lars_symp/159

Kwan, C., Ayhan, B., Budavari, B., Lu, Y., Perez, D., Li, J., Bernabe, S., & Plaza, A. 2020. Deep learning for land cover classification using only a few bands. Remote Sensing, 12(12): 2000. doi:10.3390/rs12122000

Kwan, C., Budavari, B., Bovik, A. C., & Marchisio, G. 2017. Blind quality assessment of fused WorldView-3 images by using the combinations of pansharpening and hypersharpening paradigms. IEEE Geoscience and Remote Sensing Letters, 14(10): 1835–1839. doi:10.1109/LGRS.2017.2737820

LaRocque, A., Phiri, C., Leblon, B., Pirotti, F., Connor, K., & Hanson, A. 2020. Wetland mapping with Landsat 8 OLI, Sentinel-1, ALOS-1 PALSAR, and LiDAR data in

southern New Brunswick, Canada. Remote Sensing, 12(13): 2095. doi:10.3390/rs12132095

Ma, L., Cheng, L., Li, M., Liu, Y., & Ma, X. 2015. Training set size, scale, and features in Geographic Object-Based Image Analysis of very high resolution unmanned aerial vehicle imagery. ISPRS Journal of Photogrammetry and Remote Sensing, 102: 14–27. doi:10.1016/j.isprsjprs.2014.12.026

Ma, L., Li, M., Ma, X., Cheng, L., Du, P., & Liu, Y. 2017. A review of supervised object-based land-cover image classification. ISPRS Journal of Photogrammetry and Remote Sensing, 130: 277–293. doi:10.1016/j.isprsjprs.2017.06.001

Mahdianpari, M., Salehi, B., Mohammadimanesh, F., Brisco, B., Homayouni, S., Gill, E., DeLancey, E.R., & Bourgeau-Chavez, L. 2020. Big Data for a Big Country: The First Generation of Canadian Wetland Inventory Map at a Spatial Resolution of 10-m Using Sentinel-1 and Sentinel-2 Data on the Google Earth Engine Cloud Computing Platform. Canadian Journal of Remote Sensing, 11(1): 1–19. doi:10.1080/07038992.2019.1711366

Mansourpour, M., Rajabi, M. A., & Blais, J. A. R. 2006. Effects and performance of speckle noise reduction filters on active RADAR and SAR images. International Journal of Technology And Engineering System (IJTES), 2(1): 111–114.

Marcaccio, J. V, Markle, C. E., & Chow-Fraser, P. 2015. Unmanned aerial vehicles produce high-resolution , seasonally-relevant imagery for classifying wetland vegetation. International Archives of the Photogrammetry, Remote Sensing and Spatial Information Sciences, XL-1/W4: 249–256. doi:10.5194/isprsarchives-XL-1-W4-249-2015

Marcaccio, J. V., Markle, C. E., & Chow-Fraser, P. 2016. Use of fixed-wing and multi-rotor unmanned aerial vehicles to map dynamic changes in a freshwater marsh. Journal of Unmanned Vehicle Systems, 4(3): 193–202. doi:10.1139/juvs-2015-0016

Marcaccio, J. V, & Chow-Fraser, P. 2018. Mapping invasive Phragmites australis in highway corridors using provincial orthophoto databases in Ontario. Ontario Ministry of Transportation, 1–29.

Markle, C. E., & Chow-Fraser, P. 2018. Effects of European common reed on Blanding's turtle spatial ecology. The Journal of Wildlife Management, 82(4): 857–864. doi:10.1002/jwmg.21435

Maxwell, A. E., Warner, T. A. and Fang, F. 2018. Implementation of machine-learning classification in remote sensing: An applied review. International Journal of Remote Sensing, 39(9): 2784–2817. doi:10.1080/01431161.2018.1433343.

Midwood, J. D., & Chow-Fraser, P. 2010. Mapping Floating and Emergent Aquatic Vegetation in Coastal Wetlands of Eastern Georgian Bay, Lake Huron, Canada. Wetlands, 30(6): 1141–1152. doi:10.1007/s13157-010-0105-z

Midwood, J., Rokitnicki-Wojcik, D., & Chow-Fraser, P. 2012. Development of an inventory of coastal wetlands for eastern Georgian Bay, Lake Huron. ISRN Ecology, 2012: 1–13. doi:10.5402/2012/950173

Minister of Justice, 2020. Fisheries Act. Government of Canada, Ottawa, Ontario, Canada.

Minns, C.K. & Wicheret, G.A. 2005. A framework for defining fish habitat domains in Lake Ontario and its drainage. Journal of Great Lakes Research, 31(S1): 6-27. doi:10.1016/S0380-1330(05)70287-2

Miyoshi, G. T., Arruda, M. dos S., Osco, L. P., Junior, J. M., Gonçalves, D. N., Imai, N. N., Tommaselli, A.M.G., Honkavaara, E., & Gonçalves, W. N. 2020. A novel deep learning method to identify single tree species in UAV-based hyperspectral images. Remote Sensing, 12(8): 1–18. doi:10.3390/RS12081294

Mladenova, I., & Jackson, T. J. 2011. Incidence angle normalization of backscatter data. IEEE Transactions on Geoscience and Remote Sensing, 51(3): 1791–1804. doi:10.1109/TGRS.2012.2205264

Muhammad, P., Duguay, C., & Kang, K. K. 2016. Monitoring ice break-up on the Mackenzie River using MODIS data. Cryosphere, 10(2): 569–584. doi:10.5194/tc-10-569-2016

Pekel, J. F., Cottam, A., Gorelick, N., & Belward, A. S. 2016. High-resolution mapping of global surface water and its long-term changes. Nature, 540(7633): 418–422. doi:10.1038/nature20584

Pettorelli, N., Wegmann, M., Skidmore, A. K., Mucher, S., Dawson, T. P., Fernandez, M., Lucas, R., Schaepman, M.E., Wang, T., O'Connor, B., Jongman, R.H.G., Kempeneers, P., Sonnenschein, R., Leuidner, A.K., Bohm, M., He, K.S., Nagendra, H., Dubois, G., Fatoyinbo, T., Hansen, M.C., Paganini, M., de Klerk, H.M., Asner, G.P., Kerr, J.T., Nestor Fernandez, A.B., Lausch, A., Cho, M.A., Alcaraz-Segura, D., McGeoch, M.A., Turner, W., Mueller, A., St-Louis, V., Penner, J., Vihervaara, P., Belward, A., Reyers, B., & Geller, G. N. 2016. Framing the concept of satellite remote sensing essential biodiversity variables: challenges and future directions. Remote Sensing in Ecology and Conservation, 2(3): 122–131. doi:10.1002/rse2.15

Riley, J. W., Calhoun, D. L., Barichivich, W. J., & Walls, S. C. 2017. Identifying Small Depressional Wetlands and Using a Topographic Position Index to Infer Hydroperiod Regimes for Pond-Breeding Amphibians. Wetlands, 37(2): 325-338. doi:10.1007/s13157-016-0872-2

Shuchman, R. A., Sayers, M. J., & Brooks, C. N. 2013. Mapping and monitoring the extent of submerged aquatic vegetation in the Laurentian great lakes with multi-scale satellite remote sensing. Journal of Great Lakes Research, 39(S1): 78–89. doi:10.1016/j.jglr.2013.05.006

Sibanda, M., Mutanga, O., & Rouget, M. 2017. Testing the capabilities of the new WorldView-3 space-borne sensor's red-edge spectral band in discriminating and mapping complex grassland management treatments. International Journal of Remote Sensing, 38(1): 1–22. doi:10.1080/01431161.2016.1259678

Sidhu, N., Pebesma, E., & Câmara, G. 2018. Using Google Earth Engine to detect land cover change: Singapore as a use case. European Journal of Remote Sensing, 51(1): 486–500. doi:10.1080/22797254.2018.1451782

Sidike, P., Sagan, V., Maimaitijiang, M., Maimaitiyiming, M., Shakoor, N., Burken, J., Mockler, T., & Fritschi, F. B. 2019. dPEN: deep Progressively Expanded Network for mapping heterogeneous agricultural landscape using WorldView-3 satellite imagery. Remote Sensing of Environment, 221(November 2018): 756–772. doi:10.1016/j.rse.2018.11.031

Sobiech, J., & Dierking, W. 2013. Observing lake- and river-ice decay with SAR: Advantages and limitations of the unsupervised k-means classification approach. Annals of Glaciology, 54(62): 65–72. doi:10.3189/2013AoG62A037

Surdu, C. M., Duguay, C. R., & Fernández Prieto, D. 2015. Evidence of recent changes in the ice regime of lakes in the Canadian High Arctic from spaceborne satellite observations. The Cryosphere Discussions, 9(6): 6223–6274. doi:10.5194/tcd-9-6223-2015

Traganos, D., Poursanidis, D., Aggarwal, B., Chrysoulakis, N., & Reinartz, P. 2018. Estimating satellite-derived bathymetry (SDB) with the Google Earth Engine and sentinel-2. Remote Sensing, 10(6): 1–18. doi:10.3390/rs10060859

van Duynhoven, A., & Dragićević, S. 2019. Analyzing the effects of temporal resolution and classification confidence for modeling land cover change with long short-term memory networks. Remote Sensing, 11(23): 2784. doi:10.3390/rs11232784

Wang, T., Zhang, H., Lin, H., & Fang, C. 2016. Textural-spectral feature-based species classification of mangroves in Mai Po nature reserve from WorldView-3 imagery. Remote Sensing, 8(1): 1–15. doi:10.3390/rs8010024

Wu, Q., Lane, C. R., Li, X., Zhao, K., Zhou, Y., Clinton, N., DeVries, B., Golden, H. E., & Lang, M. W. 2019. Integrating LiDAR data and multi-temporal aerial imagery to map wetland inundation dynamics using Google Earth Engine. Remote Sensing of Environment, 228: 1–13. doi:10.1016/j.rse.2019.04.015

Yang, X., Pavelsky, T. M., Allen, G. H., & Donchyts, G. 2019. RivWidthCloud: An Automated Google Earth Engine Algorithm for River Width Extraction From Remotely Sensed Imagery. IEEE Geoscience and Remote Sensing Letters, 17(2): 217-221. doi:10.1109/lgrs.2019.2920225

Ye, B., Tian, S., Ge, J., & Sun, Y. 2017. Assessment of WorldView-3 data for lithological mapping. Remote Sensing, 9(11): 1132. doi:10.3390/rs9111132

APPENDIX

Table A1. *Freely available remote sensing raw data and data products*

Name	Supplier	Data Available	Website
Airbus Sample Imagery	Airbus	SPOT data, basic elevation datasets, and radar data at specific geographic locations	intelligence-airbusds.com
ALOS World 3D	JAXA	30m resolution global DEM	eorc.jaxa.jp/ALOS/en/aw3d30
CLASS (Comprehensive Large Array-Data Stewardship System)	NOAA	Global-scale, low to moderate resolution data including MODIS	
Copernicus Scihub	European Space Agency	Sentinel-series data	scihub.copernicus.eu
DigitalGlobe Open Data	Maxar	High resolution datasets at disaster sites	digitalglobe.com/ecosystem/open-data
EarthData	NASA	Raw & real-time imagery, global-scale earth process products (e.g. climate indicators, ocean data, agriculture)	search.earthdata.nasa.gov
EarthExplorer	United States Geological Survey	Landsat satellite data, aerial imagery, and LiDAR datasets (some geo-restricted to American users)	earthexplorer.usgs.gov
EODMS (Earth Observation Data Management System)	Natural Resources Canada	Radarsat data, imagery purchased by the GoC (free to GoC employees unless authorization to new department required)	eodms-sgdot.nrcan-rncan.gc.ca
Geodiscover Alberta	Government of Alberta	Both GIS and RS products, including raw aerial imagery, image classification products, and field data	geodiscover.alberta.ca
Global Water Futures	Multiple (projects funded under GWF)	Multiple data types	gwf.usask.ca/-outputs-data/
Google Earth Engine	Multiple (collated by Google)	Pre-processed free satellite data (e.g. Landsat, Sentinel); output products such as global forest mapping & surface water mapping	earthengine.google.com
Manitoba Land Initiative	Conservation and Water Stewardship	Both GIS and RS products, including raw aerial imagery, image classification products, and field data	mli2.gov.mb.ca
Ontario GeoHub	Land Information Ontario	Both GIS and RS products, including raw aerial imagery, image classification products, and field data	geohub.lio.gov.on.ca
Saskatchewan GeoHub	Government of Saskatchewan	Both GIS and RS products, including raw aerial imagery, image classification products, and field data	geohub.saskatchewan.ca
Worldview	NASA	Similar to Google Earth; provides free image access focused on global events (e.g. widlfires, coastal erosion)	worldview.earthdata.nasa.gov

Table A2. *Commonly used remote sensing satellite-based platforms. "Data Captured" uses broader terms than specific wavelengths for easier comparison between platforms. Constellation is only included if present; spatial coverage is only listed if not worldwide between the 60th parallels*.

Name	Data Captured	Temporal Resolution	Geographic Resolution (metres/pixel)	Years of Data Available	Constellation	Owner
			Passive Sensors			
Landsat 1-3	Red, Green, NIR	18 days	60 (resampled from 79x57)	23 July 1972 - 31 March 1983		NASA
Landsat 4-5	Visible, NIR, SWIR, Thermal	16 days	30 (Thermal: 120)	16 July 1982 - 5 June 2013		NASA
Landsat 7	Panchromatic, Visible, NIR, SWIR, Thermal	16 days	30 (Thermal: 60)	15 April 1999 - present		NASA
Landsat 8	Panchromatic, Visible, NIR, SWIR, Thermal, Cirrus, Ultra blue	16 days	30 (Thermal: 100)	11 February 2013 - present		NASA
Sentinel-2	Visible, NIR, SWIR, Thermal, Red edge, Cirrus, Ultra Blue, Water Vapor	6 days	10 (Red Edge(1,2,3,4) + SWIR (1,2): 20; Ultra Blue, Cirrus, Water Vapor: 60)	23 June 2015 - present	Two	ESA
ALOS-1 / Daichi	Panchromatic, Visible, NIR	46 days (2 day sub-cycle for disaster monitoring)	10 (Visible + NIR) + 2.5 (Panchromatic)	24 January 2006 - 22 April 2011		JAXA
GOCI	Visible (6 band), 2 NIR bands	1 hour	500m	1 June 2010 - present		KOSC
ENVISAT MERIS	Visible, NIR, 15 total bands across 412nm-900nm	3 days	300m (1,000m reduced resolution)	1 March 2002 - 8 April 2012		ESA
MODIS	Cloud/Aerosols, Ocean Colour, Phytoplankton, Water Vapor, Temperature (36 total bands)	1-2 days	250m, 500m, 1,000m	24 February 2000 / 4 July 2002 (Terra / Aqua)- present	Two (Terra + Aqua)	NASA
Worldview-2	Panchromatic, Visible, two NIR bands, red edge, coastal, yellow	1-2 days	2.4m (Multispectral), 0.5m (Panchromatic)	8 October 2009 - present		

Name	Data Captured	Temporal Resolution	Geographic Resolution (metres/pixel)	Years of Data Available	Constellation	Owner
			Passive Sensors			
Worldview-3/4	Panchromatic, Visible, two NIR bands, red edge, coastal, yellow, 8 SWIR bands, 12 CAVIS bands	1-2 days	1.24m (Multispectral), 0.3m (Panchromatic), 3.7m (SWIR bands), 30m (CAVIS bands)	13 August 2014 - present	Two (Worldview-4 does not include SWIR/CAVIS bands; decommissioned in January 2019)	
GeoEye-1	Panchromatic, Visible, NIR	3 days	1.65m (Visible + NIR), 0.41m (Panchromatic)	7 October 2008 - present		DigitalGlobe
Pleiades 1	Panchromatic, Visible, NIR	1 day with constellation	2.8m (Visible + NIR), 0.7m (Panchromatic)	17 December 2011 - present	Two (Pleidas 1A + 1B); in same orbit as SPOT 6/7	
KOMPSAT/Arirang series	Panchromatic, Visible, NIR	1.4 days with constellation	4m/2.8m/2.2m (Visible + NIR; 2/3/3a), 1m/0.7m/0.55m (Panchromatic; 2/3/3a)	28 July 2006 / 17 May 2012 / 25 March 2015 - present (2/3/3a)	Two	KARI
Quickbird	Panchromatic, Visible, NIR	1-3.5 days	2.4m (Visible + NIR), 0.61m (Panchromatic)	18 October 2001 - 17 December 2014		DigitalGlobe
SkySat	Panchromatic, Visible, NIR	<1 day with constellation	1m (Visible + NIR), 0.72m (Panchromatic)	21 November 2013 - present (Gen2: 22 Jue 2016 - present)	Thirteen	Planet Labs
IKONOS	Panchromatic, Visible, NIR	3 days	3.28m (Visible + NIR), 1m (Panchromatic)	24 September 1999 - 31 March 2015		GeoEye
Gaofen series	Panchromatic, Visible, NIR	41 days	8m/3.2m (Visible + NIR; 1/2), 2/0.8m (Panchromatic; 1/2)			CNSA
TripleSat	Panchromatic, Visible, NIR	1 day with constellation	4m (Visible + NIR), 1m (Panchromatic)	10 July 2015 - present	Three	21AT
FORMOSAT series	Panchromatic, Visible, NIR	1-2 days	8m/4m (Visible + NIR; 2/5), 2m (Panchromatic)	20 May 2004/24 August 2017 (2/5) - present		NPSO Taiwan
RapidEye	Visible, NIR, Red edge	1-5.5 days with constellation	5m	28 August 2008 - present	Five	Planet Labs

Name	Data Captured	Temporal Resolution	Geographic Resolution (metres/pixel)	Years of Data Available	Constellation	Owner
			Passive Sensors			
SPOT 5	Panchromatic, Visible, SWIR		10m (Visible + NIR), 2.5m (Panchromatic)	4 May 2002 - present		CNES
SPOT 6/7	Panchromatic, Visible, NIR	1 day with constellation	6m (Visible + NIR), 1.5m (Panchromatic)	17 October 2012 - present	Two	AIRBUS
JERS-1	Green, Red, two NIR bands, 4 SWIR bands	44 days	20m	11 February 1992 - 11 October 1998	Two	JAXA
Vision-1	Panchromatic, Visible, NIR	1-8 days with constellation; 35 days (3 day for commissioning)	3.5m (Visible + NIR), 0.9m (Panchromatic)	21 November 2013 - present (Gen2: 22 Jue 2016 - present)		
Deimos-2	Panchromatic, Visible, NIR	4 days	5m (Visible + NIR), 0.75m (Panchromatic)			Deimos Imaging
Superview-1	Panchromatic, Visible, NIR	2 days	2m (Visible + NIR), 0.5m (Panchromatic)	9 January 2018 - present	Four	Beijing Space View Technology
ZiYuan-3	Panchromatic, Visible, NIR	5 days	5.8m (Visible + NIR), 2.1m (Panchromatic)	9 January 2012 - present		Ministry of Land and Resources of the People's Republic of China
OHS	32 band hyperspectral (blue to NIR)	1 day	10m	26 April 2018 - present	Eight (second set launched 19 September 2019)	Orbita
			Active Sensors			
Sentinel-1	Single polarized HH & VV, Dual Polarized with HV/VH	6 days	Full resolution: IW: 10, EW: 25 High resolution: IW&EW: 40	03 October 2014 - present	Two	
RADARSAT series	Single polarized HH & VV, Dual Polarized with HV/VH (RADARSAT-1: HH only)	14 days (less towards North Pole, e.g. 2-3 days in Arctic); Daily at 50m (RCM)	Most data in medium resolution: 30 (high: 8; low: 100)	4 November 1995 - present (RCM: 12 June 2019)	Single (RCM: 3)	CSA (RADARSAT-2)
AVHRR series	Two red bands, NIR, IR (after 1986)	1 day	1,000m	June 1979 - present		

Name	Data Captured	Temporal Resolution	Geographic Resolution (metres/pixel)	Years of Data Available	Constellation	Owner
			Active Sensors			
ALOS PALSAR series	Single polarized HH & VV, Dual Polarized with HV/VH, Quad Polarized	ALOS-1: 46 days; ALOS-2: 14 days	ALOS-1: 10m / 100m; ALOS-2: 3m, 6m, 10, 100m	24 January 2006 - 22 April 2011 (ALOS-1); 24 May 2014 - present (ALOS-2)		JAXA
ENVISAT ASAR	Single polarized HH & HV, Dual Polarized with HV/VH	3 days	30m (100m wide swath)	1 March 2002 - 8 April 2012		ESA
TerraSAR-X	Single polarized HH & HV, Dual Polarized with HV/VH	11 days (less towards poles, e.g. 3-4 days in Arctic)	1m (SpotLight), 3m (StripMap), ScanSAR(16m)	15 June 2007 - present	Two (with TanDEM-X)	Astrium
ERS series	Single VV polarized	1-8 days with constellation; 35 days (3 day for commissioning)	30m (50km in wind scatterometer mode)	17 July 1991 -10 March 2000		
JERS series	Single HH polarized	44 days	18m	11 February 1992 - 11 October 1998		JAXA
ENVISAT ASAR	Single polarized HH & VV, Dual Polarized with HV/VH	35 days (3 day for commissioning)	30m (wide swath: 150m; global monitoring: 1,000m)	1 March 2002 - 8 April 2012		ESA
KOMPSAT-5 (Corea SAR Instrument)	Single polarized HH, VV, HV, VH	28 days	1m (Highest), 3m (StripMap), 30m (global mapping)	22 August 2013 - present		KARI

Table A3. *Electromagnetic spectrum as represented in remote sensing. Active remote sensing bands are sometimes referred to by frequency in gigahertz but passive bands are not.*

Wavelength (m)	System	Colour/Name	Frequency (GHz)
$1*10^{-9}$ – $1*10^{-6}$	Passive	Ultraviolet	
$(0.4 - 0.6)*10^{-9}$	Passive	Visible	
$(0.446 - 0.500)*10^{-9}$	Passive	Blue	
$(0.500 - 0.578)* 10^{-9}$	Passive	Green	
$(0.620 - 0.700)* 10^{-9}$	Passive	Red	
$(0.7*10^{-9})$ – $(1*10^{-4})$	Passive	Infrared	
$(0.7 - 1.0)*10^{-7}$	Passive	Near Infrared	
$(1 - 1.5)*10^{-6}$	Passive	Short wave Infrared	
$(3.0*10^{-5})$ – $1*10^{-4}$	Passive	Thermal Infrared	
$(0.75 - 1.1)*10^{-2}$	Active	Ka-Band	26.5-40
$(1.1 - 1.67)*10^{-2}$	Active	K-band	18-26.5
$(1.67 - 2.4)*10^{-2}$	Active	Ku-band	12.5-18
$(2.4 - 3.75)*10^{-2}$	Active	X-band	8-12.5
$(3.75 - 7.5)*10^{-2}$	Active	C-band	4-8
$(0.75 - 1.5)*10^{-1}$	Active	S-band	2-4
$(1.5 - 3.0)*10^{-1}$	Active	L-band	1-2
$(3.0 - 10)*10^{-1}$	Active	P-band	0.3-1

Table A4. *List of commonly used remote sensing softwares. Some GIS-focused packages are included for comparison*

Software	Main functionality	Additional functionalities	Coding Language	Cloud Programming	Source
ENVI	Remote sensing	Automated Atmospheric correction, object-based image analysis, 3D point cloud generation from image data, spectra library, ESRI & DigitalGlobe & Pix4D integration, API available for custom apps, deep learning classification with extension, Additional SAR data processing capabilities with extension	IDL	Available	L3 Harris
eCognition	Object-based image analysis & remote sensing	Workflow creation, Deep learning, eCognition Server: Batch processing for large datasets		No	Trimble
ArcMap	GIS analyses	Standard GIS software tools, Workflow creation (via ModelBuilder),	Python	No	ESRI
ArcPro	GIS analyses	Standard GIS software tools, Workflow creation (via ModelBuilder),	Python	No	ESRI
Google Earth Engine	Big data remote sensing	Big data analysis, long time-series analysis	Javascript, Python	Cloud software	Google
SNAP	Sentinel satellite data processing & remote sensing			No	European Space Agency
QGIS	GIS analyses (based on GRASS & SAGA software)	Standard GIS software tools, Many plugins available e.g. semi-automatic classification	Python	No	qgis.org
ORFEO Toolbox	Remote sensing	Basic GIS software tools, Accessible via QGIS, Python, Command Line, and C++	Python	No	orfeo-toolbox.org
Pix4D	UAV image data transformation to 3D models & maps	Basic measurements (area, perimeter, volume), elevation data creation & display, machine learning-based automated image classification (aimed at agriculture & construction)	None	Available; cloud-leveraged machine learning image classification	Pix4D
DroneDeploy	UAV image data transformation to 3D models & maps	Basic measurements (area, perimeter, volume), elevation data creation & display, basic automated image classification (aimed at agriculture & construction)	None	Cloud software; third party apps available	DroneDeploy

Software	Main functionality	Additional functionalities	Coding Language	Cloud Programming	Source
Geomatica	Remote sensing	Object-based image analysis, Sentinel-1 TOPS SAR & InSAR workflows (with radar suite), Radarsat Constellation support, UAV image processing, Many additional products from PCI Geomatics to enhance usability	Python	No	PCI Geomatics
ERDAS IMAGINE	Remote sensing & GIS analyses		Python	Available	Hexagon Geospatial
Opticks	Remote sensing		Python	No	Ball Aerospace & Technologies
IDRISI/TerrSet	Remote sensing	Standard GIS software tools, Tools for REDD projects, Change detection and trends module, climate change modelling module	None	No	Clark Labs
TNTmips	GIS analyses	Standard GIS software tools, basic remote sensing tools,	SML	No	MicroImages
RemoteView	Remote sensing	Basic GIS software, SAR data integration, video analysis, object-based image analysis, LiDAR analysis, ArcGIS integration		With RVCloud integration	Overwatch Textron Systems
BEAM	Basic remote sensing	Sentinel integration (SNAP)	Java	No	European Space Agency

Table A5. *List of commonly used remote sensing techniques*

Type	Main function	Data inputs	Data outputs	Examples	FFHPP Application
Change Detection	Quantify spatial and spectral differences between images	Two raster datasets with overlapping pixels separated by a time delta	Raster data; change between images	Modeling invasive Phragmites expansion in Long Point (Jung et al. 2017)	Determine cumulative effects of physical alterations and climate change in watersheds
Image Classification, Unsupervised	Define classes within image data by their spectral properties; classes generated automatically (often by specified number of classes or minimum/maximum number of classes	Image data	Raster data; classified image	k-means classification of SAR data for lake ice delineation (Sobiech & Dierking 2013)	Fully automated image classification for initial image classification analyses to determine potential spectral distinguishability
Image Classification, Supervised	Define classes within image data by their spectral properties; reference value inputs required (training polygons or spectral values)	Image data, training polygons/spectral values	Raster data; classified image	Random forest classification for wetland type determination in Great Lakes coastal wetlands (Bourgeau-Chavez et al. 2015)	Semi-automated image classification for multiple areas of interest
Digitization	Manual delineation of features	Image data	Vector (polygon) data; no inherent properties unless user defined/calculated	Digitization of historic aerial photography to determine change over time & effects on SAR in a national park (Markle & Chow-Fraser 2018)	Easy, fully manual image classification for small areas of interest
Clustering	Create image objects with inherent spatial properties (e.g. area, perimeter, adjacent objects)	Image data	Raster or vector (polygon) data; spectral data with spatial properties	Delineation of habitat types to support coastal wetland mapping in Georgian Bay (Midwood & Chow-Fraser 2010)	Improve image classification from very high-resolution image data
			Passive data		
Band Ratios	Use a ratio of two or more bands to extract additional data on land cover features	Multi-band image raster	Raster; New ratio band	Mapping submerged aquatic vegetation with depth-invariant index (Shuchman et al. 2013)	Mapping and comparing SAV, physical habitat, vegetation vigor, soil moisture
Aerial Photography	Very high-resolution image data without atmospheric interference	Plane with orthophotography equipment, site coordinates, flight plan	Continuous image data over site, three-dimensional point cloud (if sufficient image overlap)		

Type	Main function	Data inputs	Data outputs	Examples	FFHPP Application
			Passive data		
UAV Imagery	Extremely high-resolution data with specific spectral response	UAV, site coordinates, flight plan	Continuous image data over site, three-dimensional point cloud (if sufficient image overlap)	Determine extent of invasive Phragmites in coastal wetland (Marcaccio et al. 2016)	Rapid image updates from field; very high-resolution data products
Stereoscopy	Using two overlapping images to create three-dimensional model	Overlapping image data	Three-dimensional point cloud data	Differences between stereoscopy and laser scanned point clouds (White et al. 2013	Updated surface models for more recent analysis
Spectral Power Distribution	Determine full spectral response of a feature in-situ	Spectro-radiometer data	Spectral response values	Determine Eurasian water milfoil spectral profile for wetland classification (Brooks et al. 2019)	Automated vegetation mapping using spectral profiles
			SAR data		
InSAR	Map surface deformation/elevation with high accuracy (<1m) between two dates	Two SAR images from same sensor / bands and same geometry in quick succession (time scale dependent on features imaged; <10 days)	Interferogram	Wetland water level monitoring and discrimination from other land cover types (Brisco et al. 2017)	Quantify erosion and watercourse change
Polarimetric Analysis	Define dielectric, surface, and bounceback properties of surfaces being imaged	SAR data, training polygons	N/A	Polarimetric properties of Typha wetlands (Brisco et al. 2020)	Soil moisture analyses; vegetation canopy density
DEM/DTM Generation	Use highly calibrated SAR satellite to create digital elevation model over very large areas	SAR data, reference coordinates with accurate elevation data	Rater data; DEM/DTM, DSM (vector data outputs possible)	TanDEM-X	Updated surface models for more recent analysis